Inorganic Chemistry

Article

pubs.acs.org/IC

Mixed Ligand Cu^{2+} Complexes of a Model Therapeutic with Alzheimer's Amyloid-β Peptide and Monoamine Neurotransmitters

Vijaya B. Kenche,[†,‡] Izabela Zawisza,[§] Colin L. Masters,[†] Wojciech Bal,[§] Kevin J. Barnham,[†,‡,∥] and Simon C. Drew*[,†,⊥]

[†]Mental Health Research Institute, The University of Melbourne, Victoria 3010, Australia

[‡]The Bio21 Molecular Science and Biotechnology Institute, The University of Melbourne, Victoria 3010, Australia

[§]Institute of Biochemistry and Biophysics, Polish Academy of Sciences, Warsaw, Poland

[∥]Department of Pharmacology, The University of Melbourne, Victoria 3010, Australia

[⊥]School of Physics, Monash University, Victoria 3800, Australia

Supporting Information

ABSTRACT: 8-Hydroxyquinolines (8HQ) have found widespread application in chemistry and biology due to their ability to complex a range of transition metal ions. The family of 2-substituted 8HQs has been proposed for use in the treatment of Alzheimer's disease (AD). Most notably, the therapeutic PBT2 (Prana Biotechnology Ltd.) has been shown to act as an efficient metal chaperone, disaggregate metal-enriched amyloid plaques comprised of the Aβ peptide, inhibit Cu/Aβ redox chemistry, and reverse the AD phenotype in transgenic animal models. Yet surprisingly little is known about the molecular interactions at play. In this study, we show that the homologous ligand 2-[(dimethylamino)methyl]-8-hydroxyquinoline (HL) forms a CuL complex with a conditional (apparent) dissociation constant of 0.33 nM at pH 6.9 and is capable of forming ternary Cu^{2+} complexes with neurotransmitters including histamine (HA), glutamic acid (Glu), and glycine (Gly), with glutathione disulfide (GSSG), and with histidine (His) side chains of proteins and peptides including the Aβ peptide. Our findings suggest a molecular basis for the strong metal chaperone activity of PBT2, its ability to attenuate Cu^{2+}/Aβ interactions, and its potential to promote neuroprotective and neuroregenerative effects.

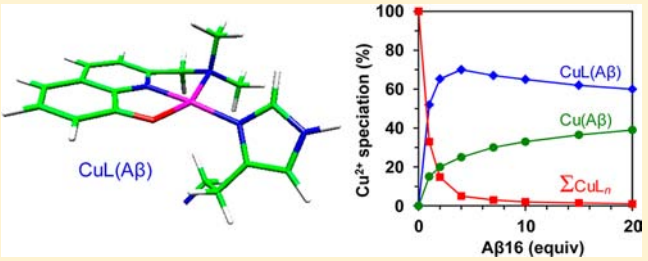

INTRODUCTION

Interest in metal chelates of 2-substituted 8-hydroxyquinolines (8HQs) began more than 40 years ago, when the ability of 2-aminomethyl-8-hydroxyquinoline (AMQ) to form stable terdentate chelates with Cu^{2+}, Ni^{2+}, Zn^{2+}, Co^{2+}, and Mn^{2+} (with stability decreasing in this order) was recognized.[1] The chelating properties of a number of other 2-substituted derivatives were subsequently studied for use as potential analytical reagents.[2] In recent years, interest in 2-susbstituted 8HQs has been rejuvenated due in large part to the potential biological applications associated with their ability to form ternary (mixed ligand) metal complexes.

Ternary metal complexes, especially those involving Cu^{2+}, have been studied for several decades as model systems for the enzyme/metal ion/substrate complexes formed during biological catalysis.[3] Such complexes consist of a metal ion coordinated to two different ligands (other than solvent). In a biological environment, these complexes predominate strongly over binary metal complexes (those consisting of metal ion coordinated to a single type of ligand), which are generally only formed when present in isolation.[3−6] Transition metal ternary complexes generally exhibit exceptionally high stability and have consequently found practical utility in the protein purification technique known as immobilized metal-ion affinity chromatography (IMAC), whereby histidine side chains form ternary metal complexes with nitrilotriacetic acid that is tethered to the column resin.[7]

Ternary metal complexes of 2-substituted 8HQs have likewise been identified for a number of biological applications. For example, the terdentate chelate of AMQ with Cd^{2+} has been proposed as an artificial guanine for sensing nucleotides involved in signal transduction (e.g., cAMP and cGMP), due to its ability to form a ternary complex with cytidine through the cooperative interaction of metal coordination and hydrogen bonding.[8] This interaction was not observed with first row transition metals such as Cu^{2+} and Zn^{2+}. Ternary metal complexes of 2-, 4-, 5-, and 7-substituted 8HQs have also been shown to form at the active site Fe^{2+} center of 2-oxoglutarate-dependent histone demethylase, leading to inhibition of enzyme activity and perturbed transcriptional regulation.[9] While the previous two examples may have direct epigenetic consequences, other applications of 2-substituted 8HQs require that their metal complexes be inert in order that they can be

Received: October 18, 2012
Published: March 28, 2013

   dx.doi.org/10.1021/ic302289r | Inorg. Chem. 2013, 52, 4303−4318

used as medical imaging agents without perturbing neurophysiology.[10] Further alternative applications presuppose such ligands actively sequester and redistribute extracellular metal ions within the central nervous system (CNS),[11] and 2-substituted 8HQs are being examined as therapeutics for the treatment of neurodegenerative conditions including Alzheimer's disease (AD), where a metal ion imbalance is proposed to exist in the brain.[12] In particular, the compound PBT2 has been shown to significantly reduce neuropathological AD markers in transgenic animal models[13,14] and provide a significant improvement over placebo in two executive function component tests of a neuropsychological test battery within a phase IIa clinical trial.[15] Such effects have been proposed to result from the ability of PBT2 to facilitate intracellular copper uptake.[13−15]

PBT2 is an 8HQ containing an exocyclic amine and is homologous to the compound 2-[(dimethylamino)methyl]-8-hydroxyquinoline (HL) shown in Scheme 1.[16−18] The

Scheme 1

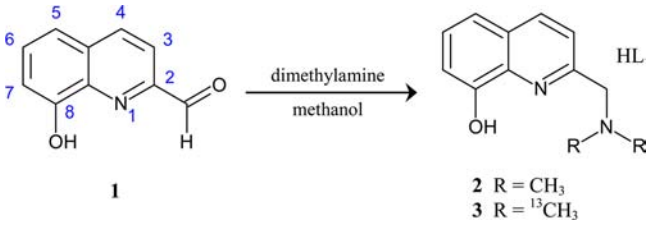

ionophore activity of PBT2 is superior to other 8HQ compounds that lack 2-substitution, such as 5-chloro-7-iodo-8-hydroxyquinoline (CQ).[11,19−24] However, to date, little consideration has been given to the variety of ternary metal complexes that PBT2 and similar compounds may form with biological cofactors. An exception is the proposition that they may form a ternary Cu^{2+} (or Zn^{2+}) complex with the β-amyloid (Aβ) peptide from which the characteristic AD plaques are formed.[11,13,25,26] Although it is well established that Aβ will form ternary complexes with Cu and small ligands such as buffer molecules,[27] to date no direct evidence for ternary interaction with PBT2 has appeared in the literature.

Given that copper homeostasis is dysregulated in AD[11,12,23,24] and high concentrations of Cu (at least 15 μM[28] and as high as 250 μM[29]) are estimated to be released during neurotransmission, we sought to determine whether the prototypical compound L can form ternary Cu^{2+} complexes, specifically with Aβ and neurotransmitters. In this study, we therefore examined the Cu^{2+} coordination of L using continuous wave (CW) and pulsed electron paramagnetic resonance (EPR) spectroscopy, isotopic labeling, and density functional theory (DFT). We demonstrate that, in contrast to ordinary 8HQs such as oxine and CQ, L can adopt both bidentate and terdentate coordination *via* its phenolato, imino, and exocyclic amino groups to form distorted square planar and square pyramidal complexes, CuL, and CuL_2, respectively. Upon introduction of competing physiological ligands such as the neurotransmitter histamine (HA), His, or protein-based histidine side chains (e.g., Aβ), terdentate L forms ternary CuLX complexes with the monodentate ligand X coordinating *via* its imidazole nitrogen. Additional ternary CuLY complexes are formed with neurotransmitters Y = glutamate (Glu) and glycine (Gly), and with oxidized glutathione (GSSG), each involving bidentate coordination of both L and Y in a distorted square planar geometry. Tryptamine- and tyramine-based neurotransmitters (e.g., serotonin, melatonin, dopamine), and also the inhibitory neurotransmitter γ-aminobutyric acid (GABA), which lack the carboxylato moiety of tryptophan (Trp), tyrosine (Tyr), and Glu, respectively, do not form stable ternary complexes. The identified ternary interactions involving Cu^{2+}, Aβ, HA, Glu, Gly, and GSSG suggest a molecular-level explanation of PBT2's strong ionophore activity, its ability to reduce neuropathological AD markers in transgenic animal models, and its cognitive efficacy in certain executive function tests in AD patients.

EXPERIMENTAL SECTION

Synthesis. Aβ1−16 (DAEFRHDSGYEVHHQK−OH) and Aβ6−14 (HDSGYEVHH) were prepared by solid phase peptide synthesis using standard protocols as described previously.[30−32] α-Synuclein (α-Syn) was expressed and purified as described earlier.[33] Synthesis of the 8-hydroxyquinolines was according to Scheme 1.[18]

*2-Formyl-8-hydroxyquinoline (**1**).* This compound was prepared according to the procedure published by Hassani et al.[34]

*2-[(Dimethylamino)methyl]-8-hydroxyquinoline (**2**).* A mixture of 2-formyl-8-hydroxyquinoline (**1**) (1 mmol) and 2 M solution of dimethylamine/methanol (2 mL) in methanol (3 mL) was stirred overnight at room temperature. The reaction mixture was cooled in an ice-bath and treated with sodium borohydride (20 mg), and then stirred at the same temperature for another 2 h. The reaction was quenched with aqueous 1 M HCl (1 mL) and extracted with dichloromethane (2 × 30 mL). The organic layers were combined, washed with brine, and dried over Na_2SO_4. After concentrating *in vacuo*, the residue was subjected to column chromatography (silica gel, 0.1:10:90 of NH_4OH/methanol/dichloromethane) to isolate the required product **2** (180 mg). The free base was treated with 1 M HCl in methanol to give its hydrochloride salt. ^{1}H NMR (500 MHz, DMSO): δ 10.64 (bs, 1H), 9.92 (bs, 1H), 8.42 (d, J = 8.4 Hz, 1H), 7.55 (d, J = 8.4 Hz, 1H), 7.46 (dd, J = 8, 7.5 Hz, 1H), 7.43 (dd, J = 8.1, 1.1 Hz, 1H), 7.13 (dd, J = 7.5, 1.1 Hz, 1H), 4.73 (d, J = 5 Hz, 2H), 2.90 (d, J = 4.6 Hz, 6H); MS m/z 203.12 (M + H).

The ^{13}C labeled compound **3** was prepared using the above procedure. ^{1}H NMR (500 MHz, DMSO): δ 10.4 (bs, 1H), 9.86 (s, 1H), 8.42 (d, J = 8.5 Hz, 1H), 7.55 (d, J = 8.5 Hz, 1H), 7.48 (dd, J = 8, 7.5 Hz, 1H), 7.43 (dd, J = 8, 1.2 Hz, 1H), 7.14 (dd, J = 7.5, 1.2 Hz, 1H), 4.73 (s, 2H), 2.90 (d, J = 143.2 Hz(^{13}C−H coupling), 6H). MS m/z 205.12 (M + H).

Sample Preparation. A full list of the ligands utilized in this study is given in Scheme 2. L was solubilized in DMSO at a concentration of 100 mM and then diluted in MQ water to a stock concentration of 1 mM. Lyophilized Aβ1−16 (Aβ16) peptides were suspended in phosphate buffered saline (PBS; 10 mM phosphate buffer, 2.7 mM KCl, 137 mM NaCl; Sigma) at concentration of 1−2 mM, as determined using ε_{280} = 1280 M^{-1} cm^{-1}. Lyophilized Aβ6−14 was resuspended in PBS at a concentration of ∼200 μM assuming ε_{280} = 1280 M^{-1} cm^{-1}. $^{65}CuCl_2$ was prepared by stirring ^{65}CuO (^{65}Cu > 99%; Cambridge Isotope Laboratories) in concentrated HCl, continuously boiling off the excess HCl, and diluting in Milli-Q water. $^{65}CuSO_4$ was prepared by stirring ^{65}CuO in 4 equiv of 98% w/w H_2SO_4 at 60 °C. All amino acids and neurotransmitters were purchased from Sigma-Aldrich and prepared as concentrated stock solutions in PBS. $^{13}C_3$-Glycerol (99% ^{13}C) was purchased from Sigma-Aldrich. The stock solutions were then combined in the desired molar ratio to a final volume of 200 μL and a typical final L concentration of 220 μM for CW-EPR and 450 μM for pulsed EPR. For ^{17}O water studies, the aqueous solution was dried by evaporative centrifugation and reconstituted in an equivalent volume of $H_2{}^{17}O$ (90% ^{17}O, Aldrich). EPR samples had an additional 10% v/v glycerol added as a cryoprotectant. The final solution pH was measured using a microprobe (Hanna Instruments, Italy) and adjusted using concentrated NaOH or HCl as required. In the case of ^{17}O water studies, the pH was adjusted prior to reconstitution in $H_2{}^{17}O$ and glycerol

dx.doi.org/10.1021/ic302289r | Inorg. Chem. 2013, 52, 4303−4318

Scheme 2. Ligands Utilized in This Study[a]

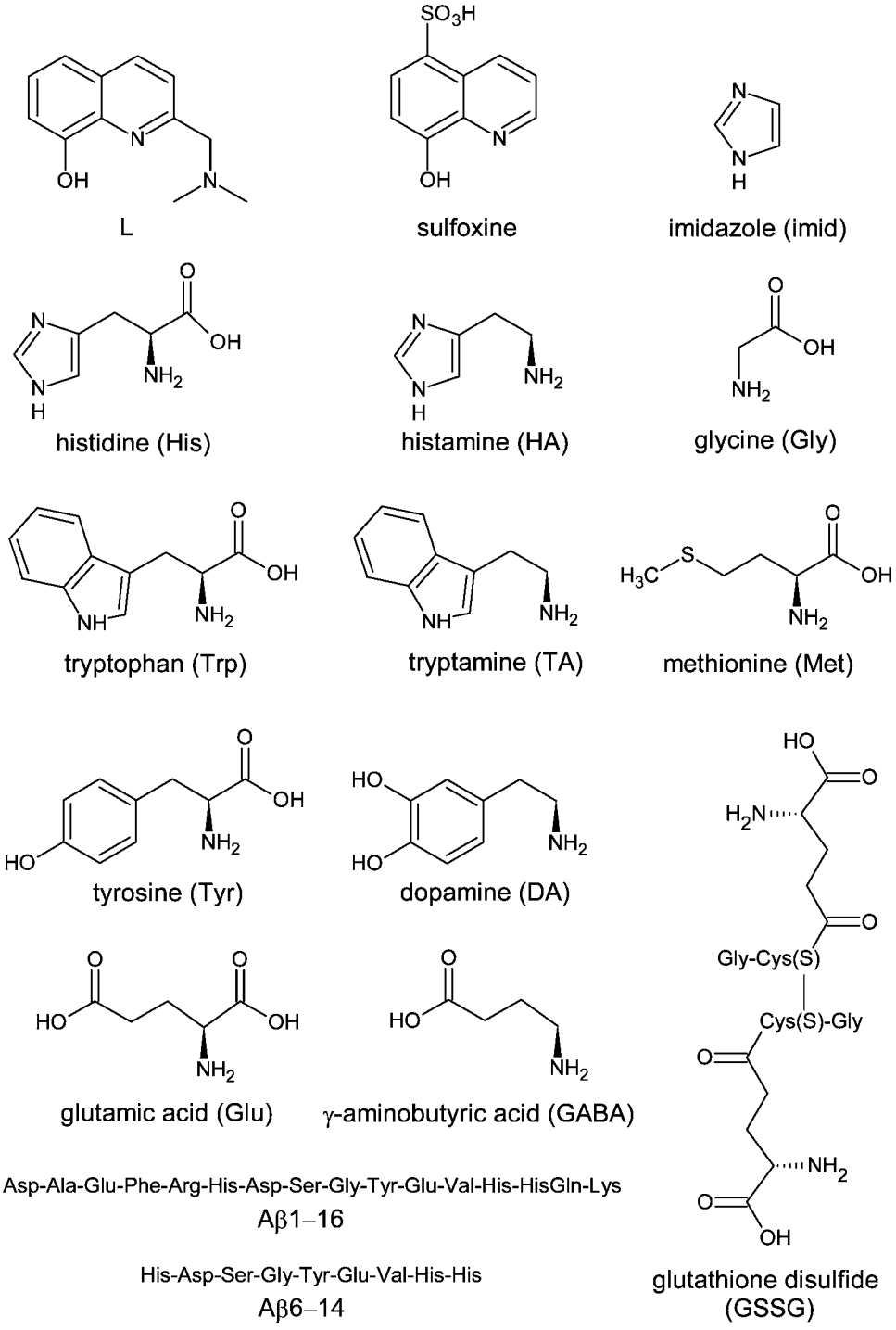

[a]For comparison, the structure of PBT2 may be found in ref 17.

addition. EPR samples were transferred to quartz tubes (Wilmad, SQ-707-250M) and snap frozen in liquid nitrogen. In all cases throughout the text, "Cu" refers exclusively to the divalent oxidation state. Unless otherwise stated, $^{65}CuCl_2$ was used, and the buffer was PBS pH 6.9.

CW-EPR Spectroscopy. X-band (9.45 GHz) CW-EPR spectra were obtained using a Bruker E500 spectrometer fitted with a Bruker superhigh-Q microwave cavity and a quartz coldfinger insert (Wilmad, WG-816-B-Q). The magnetic field was calibrated using the g factor of the BDPA radical as a reference.[35] Unless otherwise indicated, experimental conditions were as follows: microwave power, 10 mW; magnetic field modulation amplitude, 8 G; field modulation frequency, 100 kHz; receiver time constant, 328 ms; receiver gain, 10^5; sweep rate, 6.67 G s^{-1}; typical number of averages, 4. Background correction was performed by subtraction of a third order polynomial. Spin Hamiltonian parameters ($g_{||}$, $A_{||}$, etc.) of each coordination mode were determined from numerical simulations of the CW-EPR spectra using version 1.1.4 of the XSophe-Sophe-XeprView computer simulation software[36] on an i686 PC running Mandriva 2007, as described in detail in earlier studies.[30]

Spectral deconvolutions were performed as described in ref 33. In the present study, spectra of the relevant ternary species were first isolated by weighted subtraction of spectra corresponding to CuL,

dx.doi.org/10.1021/ic302289r | Inorg. Chem. 2013, 52, 4303–4318

CuL_2, and other binary Cu^{2+} complexes. All isolated ternary and binary spectra were then normalized by their respective double-integrated intensities. Spectra comprising mixtures of Cu^{2+} species were then empirically reproduced by adding linear combinations of normalized binary and ternary EPR spectra and adjusting relative weightings to minimize the difference between the empirical reconstruction and the experimental spectrum. Fitting was guided by minimization of the mean-squared deviation between the reconstruction and the experimental spectrum.

Pulsed EPR Spectroscopy. Superhyperfine (shf) interactions between Cu^{2+} and remote, noncoordinating nuclei were measured using the electron spin echo envelope modulation (ESEEM) method at X-band (9.70 GHz) using a Bruker ESP380E spectrometer fitted with a Bruker ER 4118 dielectric resonator, an Oxford Instruments CF935 cryostat with an ITC4 temperature controller, and a 1 kW TWT amplifier. Two-dimensional hyperfine sublevel correlation (HYSCORE) experiments were carried out at 15 K using a $\pi/2-\tau-\pi/2-t_1-\pi-t_2-\pi/2-\tau$-echo sequence comprising pulse lengths of $t_{\pi/2}$ = 16 ns and t_π = 24 ns. A 4-step phase cycle was used to eliminate unwanted echoes. For ^{13}C HYSCORE experiments, the time intervals t_1 and t_2 were varied from 48 to 8176 ns in steps of 64 ns (Nyquist frequency of 7.81 MHz); a value of τ = 144 ns was used to prevent blind spots below 7 MHz and to suppress the frequency foldback of signals near ν_H (proton Larmor frequency) arising from small ^1H couplings.[37] In all spectra, the real part of the time-domain quadrature signal was selected, background corrected in both dimensions using a low-order polynomial fit, zero-filled to 256 × 256 data points, and apodized with a Hamming window function. Lastly, a two-dimensional fast Fourier transformation was performed and the final spectrum obtained upon absolute value calculation.

UV−Vis Spectrophotometry. Electronic absorption spectra were obtained between 200 and 1000 nm with either a DU 730 spectrophotometer (Beckman Coulter) or a SPECTROstar *Nano* (BMG LABETCH) using a 50 μL quartz cuvette with a 1 cm path length.

Potentiometry. Potentiometric titrations were performed on a Titrando 907 automatic titrator (Metrohm), using InLab 422 combined glass-Ag/AgCl electrodes (Mettler-Toledo), which were calibrated daily by nitric acid titrations.[38] A 0.1 M NaOH solution (carbon dioxide free) was used as titrant. Sample volumes of 1.2−1.5 mL were used. The samples contained 1.0 mM L, dissolved in 4 mM HNO_3/96 mM KNO_3. The Cu^{2+} complex formation was studied using a 4-fold molar excess of L over Cu^{2+}, added as $Cu(NO_3)_2$. All experiments were performed under argon at 25 °C, in the pH range 2.3−12.2. The collected data were analyzed using the HYPERQUAD program.[39] Three titrations were included simultaneously into calculations, separately for protonation and Cu^{2+} complexation.

Theoretical Calculations. Starting structures for optimization were manually drawn using ACD/Chemsketch version 12.01 (Advanced Chemistry Development Inc., Ontario, Canada). The starting geometries were then optimized in redundant internal coordinates using the ORCA package[40] using the spin-unrestricted Kohn−Sham (UKS) formalism in conjunction with the conductor-like screening model (COSMO) and water as the solvent. At each optimization step, the UKS equations were solved self-consistently using the BP86 GGA functional incorporating Becke 88 exchange[41] and the Perdew 86 correlation.[42] A TZVP basis comprising Alrichs-TZV[43] and Alrichs polarization functions[44] were used for all atoms except H, where Alrichs VDZ basis[43] and Alrichs polarization functions was used.[44] The self-consistent field calculations employed the resolution of the identity (RI) Coulomb approximation implemented in ORCA using a suitable TZVP auxiliary basis constructed automatically by the program. Convergence criteria for geometry optimization (in atomic units) were as follows: energy change, 5×10^{-6} hartree/bohr; maximum gradient, 3×10^{-4} hartree/bohr; RMS gradient, 1×10^{-4} hartree/bohr; maximum displacement, 4×10^{-3} bohr; RMS displacement, 4×10^{-3} bohr. All other parameters including integration grid sizes and accuracy, and COSMO terms, were the ORCA defaults. Molecular structures were rendered for display using gOpenMol.[45]

RESULTS

Cu^{2+} Binding Stoichiometry and Coordination of L. The UV−vis spectrum of a solution of L in PBS pH 6.9 was characterized by absorption maxima at approximately 240 nm and 310 nm due to ligand-centered (LC) charge-transfer bands arising from $\pi-\pi^*$ and $n-\pi^*$ transitions, respectively (Figure 1,

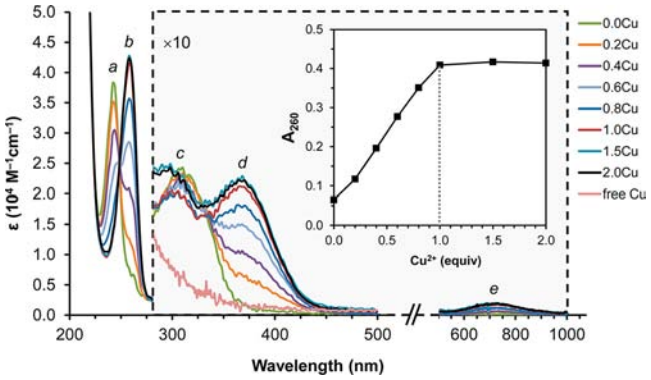

Figure 1. UV−vis absorption spectra of L, following the titration of 0−2 equiv $CuCl_2$. The inset shows absorbance at 260 nm as a function of $CuCl_2$ addition. The dashed box corresponds to the spectrum obtained at [L] = 100 μM, while the shorter wavelength spectra were acquired at [L] = 10 μM. Beyond 1 equiv $CuCl_2$, aqueous Cu^{2+} contributes an additional broad absorbance below 400 nm that is most evident at position c ("free Cu" spectrum was obtained at $[Cu^{2+}]$ = 50 μM in absence of L). Extinction coefficients: ε^{L}_{242} ($\pi\rightarrow\pi^*$) = 38 000 M^{-1} cm^{-1}, ε^{L}_{310} ($n\rightarrow\pi^*$) = 2450 M^{-1} cm^{-1}, ε^{CuL}_{260} = 41 000 M^{-1} cm^{-1} (LMCT), ε^{CuL}_{365} = 2100 M^{-1} cm^{-1} (LMCT), $\varepsilon^{CuL}_{720} \approx$ 190 M^{-1} cm^{-1} (d−d).

positions a and c). In addition to metal-centered d−d transitions near 720 nm (position e), titration of $CuCl_2$ into the solution of L elicited hypochromic shifts of the LC charge-transfer bands and hyperchromic shifts of ligand-to-metal charge transfer (LMCT) transitions at 260 nm (position *b*) and 365 nm (position *d*), with corresponding isosbestic points near 250 nm and 335 nm. The electronic spectra in Figure 1 were very similar to those reported for other 8HQs such as oxine and CQ.[46] However, compared with these 8HQs, which preferentially bind 0.5 equiv Cu^{2+} in a bis complex,[46,47] the intensity of the absorption bands at 260, 365, and near 720 nm saturated at 1.0 equiv Cu^{2+}, indicating L could coordinate Cu^{2+} in a 1:1 complex. The sharp end point of the titration indicated the Cu^{2+} binding was tight ($K_d \ll \mu M$) at the concentrations used and hence that UV−vis spectrophotometry was unsuitable for the determination of Cu binding constants. The stability constants were therefore measured by potentiometric titration. At 25 °C and an ionic strength of I = 0.1 M (KNO_3), the cumulative (log β) stability constants of CuL and CuL_2 complexes were determined to be 14.21 ± 0.02 and 22.53 ± 0.02, respectively, with an apparent dissociation constant for CuL of 3.3×10^{-10} at pH 6.9 and 3.5×10^{-11} at pH 7.4 (Table S1, Supporting Information). In comparison, the mono and bis Cu complexes of oxine have reported cumulative stability constants of 12.2 and 23.4, respectively.[48] Thus, consistent with similar studies of the closely related AMQ ligand,[1] the CuL species is stabilized while the CuL_2 complex is destabilized by the presence of the exocyclic amine, relative to unsubstituted 8HQ ligands.

A titration of $^{65}CuCl_2$, monitored by CW-EPR, yielded spectra comprised of three distinct "type II" Cu^{2+} species

dx.doi.org/10.1021/ic302289r | Inorg. Chem. 2013, 52, 4303−4318

(Figure 2). Quantification of the total Cu^{2+} bound by double-integration of the spectra again indicated that the complex

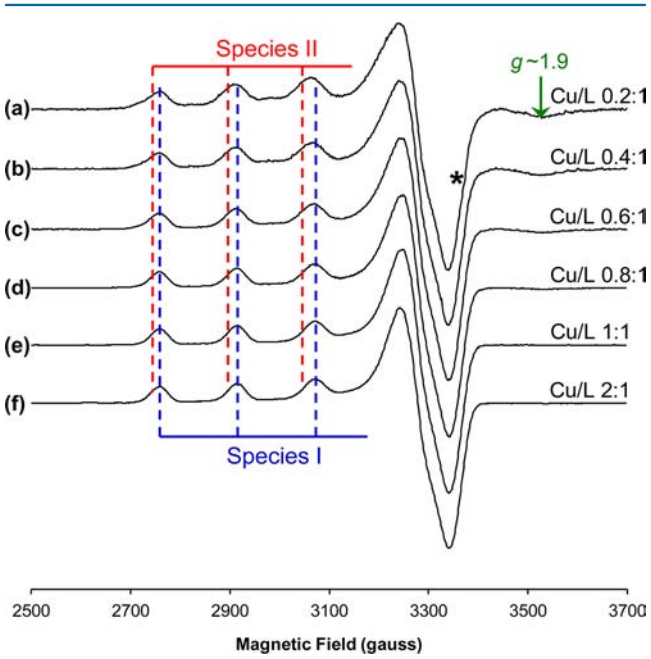

Figure 2. (a–f) X-band (9.45 GHz) CW-EPR spectra of L obtained with increasing $^{65}CuCl_2$ additions and [L] = 220 μM. The main features corresponding to the principal $g_{\|}$ and $A_{\|}(^{65}Cu)$ parameters of each species are marked by dashed vertical lines. At low Cu/L ratios, a second coordination mode ascribed to the bis complex CuL_2 is visible (species II). Other features include a high-field signal characteristic of spin-coupled Cu^{2+} dimers (species III) due to π-stacking interactions of neighboring CuL_2 complexes (arrow), and a very minor species indicative of a stable ligand-centered radical (asterisk). To aid comparison, all spectra are scaled to have the same peak-to-peak intensity. An exceedingly weak signal due to aqueous (hydrated) Cu^{2+} is evident at Cu/L ratios > 1.0 (lowest field hyperfine line near 2600 G); however, the majority of the aqueous Cu^{2+} precipitates as EPR-silent copper hydroxide at pH 6.9. A complete Cu titration is provided in Figure S3 (Supporting Information).

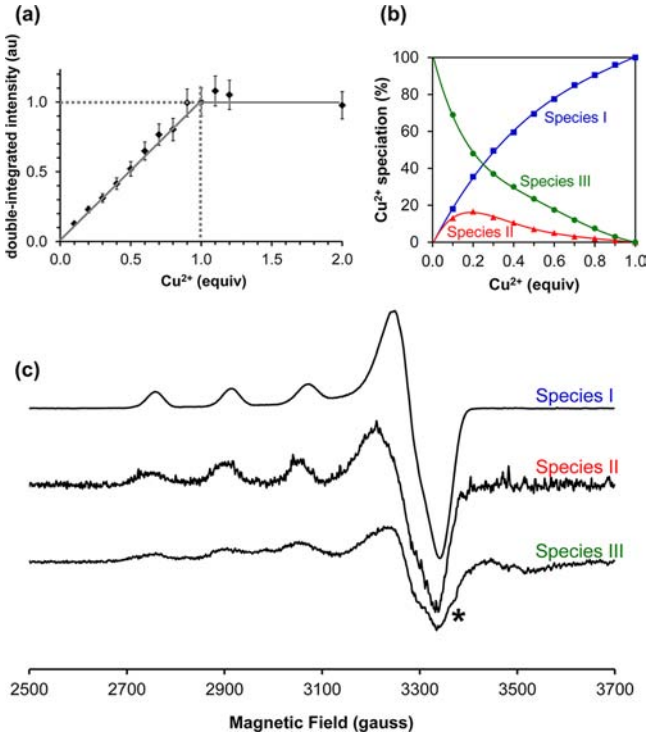

Figure 3. (a) Absolute signal intensities obtained from double-integration of the CW-EPR spectra of Figure 2, showing saturation of binding at 1 equiv $CuCl_2$. Error bars depict ±10% of the calculated intensity and reflect typical uncertainty in quantifying the concentration of paramagnetic species by CW-EPR. Lines are a guide to the eye. (b) Distribution diagram of complexes formed by Cu/L 1:*n* (*n* = 1–10). Lines are a guide to the eye and are extrapolated to $[Cu^{2+}] = 0$. (c) CW-EPR spectra of isolated CuL (species I), CuL_2 (species II), and π-stacked CuL_2 (species III), each normalized by their double-integrated intensity. The residual species indicated by the asterisk is due to the ligand-centered radical.

formation between Cu^{2+} and L is complete upon binding 1 equiv (Figure 3a). In the presence of 1 equiv of $^{65}Cu^{2+}$, a single coordination mode was present (species I), which was ascribed to a 1:1 complex, CuL. At low Cu^{2+} stoichiometry, additional species could be identified: (i) species II, attributable to a bis complex of the form CuL_2; (ii) a broad signal at an effective *g* value of 1.9 (species III), diagnostic of a spin-coupled dimeric species arising from Cu^{2+} centers being brought into proximity;[49−51] (iii) a narrow signal at an effective *g* value of 2.005, consistent with a ligand-centered radical (Figure 2). The radical, which was present even in the absence of added Cu^{2+} (not shown), represents an insignificant fraction of the total paramagnetic species present (determined by double-integration of the EPR intensity) and will not be discussed further. The linearity of the Cu^{2+} titration (Figure 3a) and saturation of the double-integrated EPR intensity at 1.0 equiv Cu^{2+} indicated that there were no EPR-silent spin-coupled $S = 1$ species with very large antiferromagnetic exchange interactions between neighboring Cu^{2+} centers. In a 50% aqueous ethanol solution (with 10 mM PBS), conditions under which π aromatic bonds are disrupted, species III disappeared, indicating that the dimer interaction is mediated by aromatic π stacking of neighboring Cu^{2+}-bound molecules.[51] Since the dimer is not observed at stoichiometric ratios of Cu^{2+} and L (where only CuL is present), the coupling of neighboring Cu^{2+} centers must be mediated by π stacking of CuL_2 species. Intermolecular π-stacking interactions have been observed for other Cu^{2+} and Zn^{2+} bound 8HQs in the solid state,[47] and we also observed a dimeric signal near $g \sim 1.9$ in the frozen solution EPR spectra of for $Cu(sulfoxine)_2$ (Figure S1, Supporting Information).

On the basis of the binding stoichiometry, terdentate Cu^{2+} coordination of L was expected for species I (CuL). To more firmly establish the identity of the coordination sphere of the 1:1 complex, HYSCORE spectroscopy was performed using an isotopically labeled analogue of L, with site specific ^{13}C-labeling of the methyl carbon nuclei. ^{13}C-HYSCORE revealed correlation ridges centered upon the ^{13}C Larmor frequency (Figure 4a) with a splitting consistent with the presence of ^{13}C nuclei two bonds from Cu^{2+},[30−32,52] confirming the coordination of the excocyclic amine of L and being consistent with the expected terdentate coordination of this class of ligand.[1] Notably, when the number of equivalents of Cu^{2+} was reduced from 1.0 to 0.5, such that a significant amount of species II (CuL_2) was also present, the intensity of ^{13}C cross peaks remained comparable after correcting for absolute Cu^{2+} concentration (Figure 4b), indicating terdentate coordination is also adopted in species II (species III was not present since relaxation times are significantly shortened due to dipolar Cu^{2+} interactions). The principal $g_{\|}$ and $A_{\|}(^{65}Cu)$ parameters of

dx.doi.org/10.1021/ic302289r | Inorg. Chem. 2013, 52, 4303−4318

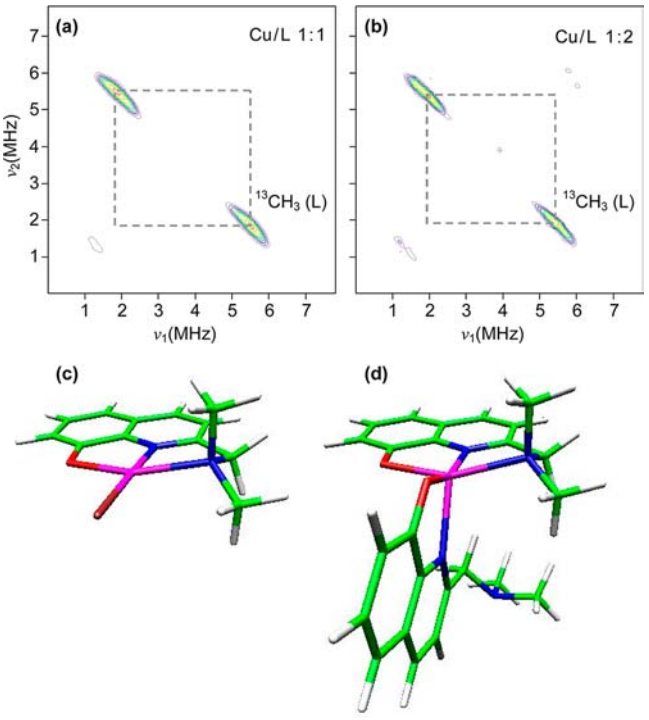

Figure 4. (a, b) X-band (9.70 GHz) HYSCORE spectra (τ = 144 ns) of Cu/L 1:1 and Cu/L 1:2, obtained at 3370 G (near $g_\perp$). The ^{13}C correlation ridges centered upon the ^{13}C Larmor frequency with a splitting of ca. 3.6 MHz confirm the coordination of the exocyclic amine in both instances. (c, d) Energy-optimized structures satisfying the constraints imposed by CW-EPR and HYSCORE, with CuL (species I) involving terdentate coordination of L with Cl^- binding and CuL_2 (species II and III) involving terdentate and bidentate coordination in a 5-coordinate bis complex. Color definitions: pink, Cu^{2+}; brown, Cl; blue, N; green, C; red, O; white, H.

species I (Table 1) were consistent with terdentate coordination of L by 2N and 1O, along with an additional

Table 1. Spin Hamiltonian Parameters Characterizing Selected Binary and Ternary Cu^{2+} Complexes at pH 6.9

complex	$g_\parallel$	$g_\perp$	$A_\parallel(^{63}Cu)^a$
CuL[b]	2.255 ± 0.001	2.055 ± 0.001	153 ± 1
CuL_2[c]	2.267 ± 0.001	2.061 ± 0.001	149 ± 1
CuLX; X = -xx-His-yy-, His, HA, imid[d]	2.245 ± 0.001	2.051 ± 0.001	145 ± 1
CuLY; Y = Glu, Gly, Trp, Tyr, Met, GSSG, xx[e,d]	2.260 ± 0.003	2.052 ± 0.003	180 ± 3
Cu(Aβ)[f]	2.272 ± 0.005	2.056 ± 0.005	171 ± 3

[a]All hyperfine parameters are expressed in units of 10^{-4} cm^{-1} (1×10^{-4} cm^{-1} = 2.9979 MHz). To aid comparison with natural abundance copper spectra (69% ^{63}Cu, 31% ^{65}Cu), hyperfine couplings have been converted from ^{65}Cu to those expected for ^{63}Cu using the scaling factor $|g_n(^{65}Cu)/g_n(^{63}Cu)| = 1.07$. [b]Species I. [c]Species II. [d]xx, yy = any amino acids. [e]Uncertainties in parameters encompass the estimated range of values observed for different amino acids. [f]Taken from ref 30.

equatorial ligand, possibly water.[53,54] To determine whether the remaining equatorial ligand of species I was in fact water, ^1H-HYSCORE spectra were also obtained. Surprisingly, no ^1H correlation ridges (centered on the ^1H Larmor frequency) expected for equatorial water coordination[55] could be discerned (data not shown). Moreover, Cu/L 1:1 prepared in 90% $H_2{}^{17}O$ also revealed none of the expected spectral broadening of the hyperfine structure in the CW-EPR spectrum due to the coupling of an equatorially coordinated ^{17}O nucleus ($I = {}^5/_2$; g_n = −0.7575)[56] (Figure S2a,b, Supporting Information). Elimination of the cryoprotectant from the solution did not significantly affect the CW-EPR spectrum (Figure S2c, Supporting Information), and HYSCORE spectroscopy using ^{13}C-glycerol further revealed only a diagonal peak at the ^{13}C Larmor frequency due to remote glycerol solvent ions (data not shown). Hence, oxygen coordination by glycerol, which is known to occur in some circumstances,[57] was not interfering. The 1:1 complex was also prepared in 10 mM MOPS buffer containing 150 mM NaCl (Figure S2d, Supporting Information). Again, the CW-EPR spectrum was unchanged, indicating that phosphate anions were not required for the formation of species I. However, elimination of NaCl from either 10 mM MOPS or 10 mM phosphate buffer (PB) had a significant impact on the spectrum, and in the case of PB, gradual reduction of the NaCl concentration appeared to shift the equilibrium from pure species I to a mixture also containing species II (Figure S2e−k, Supporting Information). Since the reduction in ionic strength can increase the pK_a of the coordinating groups of L by approximately 0.5 units,[58] we also substituted NaCl in the PB with NaF. In this instance, a spectrum similar to that observed in the absence of NaCl was obtained (Figure S2l, Supporting Information), confirming that the decrease in species I upon reducing [NaCl] was due to the direct role of chloride ions in CuL rather than changes in ionic strength. These cumulative observations supported the assignment of a CuL(Cl) coordination sphere for species I, denoted CuL for brevity. It is worth noting that the persistence of an EPR signal from CuL(Cl), even in the absence of added NaCl, was in principle possible because L was synthesized as its hydrochloride salt. Geometry optimization of CuL using DFT produced the structure shown in Figure 4c.

Isolation of the CW-EPR spectra corresponding to species II and III could be achieved by making use of the spectrum obtained in 50% aqueous ethanol, which eliminated species III (Figure S4, Supporting Information). The absence of species II in PBS pH 6.9 when equimolar Cu^{2+} was present indicated there is little stability to be gained in forming this species, which was logically ascribed to the CuL_2 complex based upon the stability constants determined from the potentiometric data (*vide supra*). Examination of a number of alternative coordination geometries by DFT (Figure S5, Supporting Information) indicated that hexacoordinate CuL_2, wherein both ligands are terdentate, produced the highest energy structure, while the most stable bis complex was a 5-coordinate distorted square pyramidal structure that maintains terdentate coordination of the first L, while the second L coordinates in a bidentate axial/equatorial fashion (Figure 4d). This structure is consistent with the ^{13}C-HYSCORE data of Figure 4, which indicates that terdentate coordination of L persists at lower Cu/L stoichiometries where CuL_2 is populated. The structure is also in accordance with the much lower log β associated with coordination of the second L (log β_2 = 8.3 vs log β_1 = 14.2).

Following isolation of species I−III, the spectra in Figure 2a−f could be deconvoluted (Figure S6, Supporting Information) and a distribution diagram generated, which is shown in Figure 3b. In physiological buffer, species I predominates at Cu/L ratios >0.3, species III is seen to monotonically increase with decreasing Cu/L ratios, and species II is a minor component at all stoichiometries. The isolated spectra of species I−III are shown in Figure 3c.

dx.doi.org/10.1021/ic302289r | *Inorg. Chem.* 2013, 52, 4303−4318

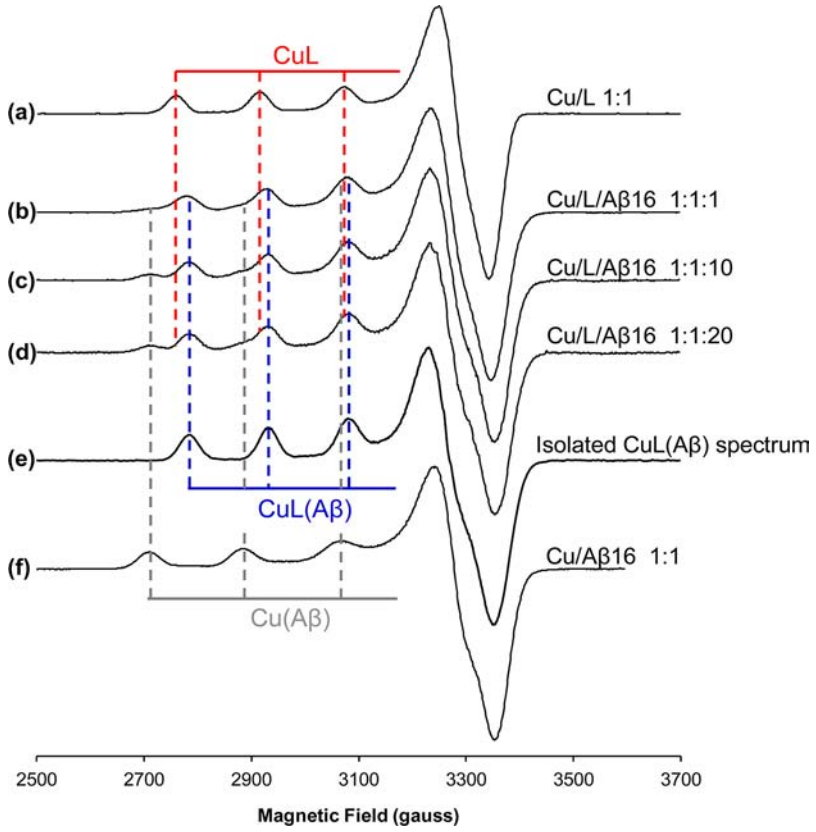

Figure 5. X-band (9.45 GHz) CW-EPR spectra of Cu/L/Aβ 1:1:*n* showing the formation of a ternary complex upon titrating 1−20 equivalents Aβ16 into equimolar Cu/L. (a) Cu/L 1:1, (b) Cu/L/Aβ 1:1:1, (c) Cu/L/Aβ 1:1:10, (d) Cu/L/Aβ 1:1:20, (e) CuL(Aβ) spectrum, isolated as shown in Figure S7 (Supporting Information), (f) Cu/Aβ 1:1. Vertical dashed lines indicate the positions of the resolved $A_{\|}$(^{65}Cu) hyperfine lines for each species; for clarity, only CuL is indicated, although CuL_2 species are also present. To maintain practical Aβ concentrations at higher stoichiometries, spectra b and c−d were acquired with a total Cu^{2+} concentration of 225 μM and 110 μM, respectively. A complete Aβ titration is provided in Figure S8 (Supporting Information).

Cu^{2+} Coordination of Mixtures of L and Aβ. To determine how L may modulate Cu^{2+}/Aβ interactions, 1−20 equiv of Aβ16 were titrated into an equimolar mixture of Cu/L. As shown in Figure 5, the EPR spectra contained signals corresponding to CuL and the binary CuL_2 and Cu(Aβ) complexes. An additional signal emerged with increasing Aβ concentration, assigned to a unique ternary CuL(Aβ) species. Using weighted spectral subtractions, the spectrum of the ternary species could be isolated (Figure S7, Supporting Information), which is shown in Figure 5e. Using the spectra of Cu(Aβ), CuL(Aβ), CuL (species I), and CuL_2 (species II−III) as a basis, the spectra of Cu/L/Aβ 1:1:*n* (*n* = 1−20) could be deconvoluted (Figure S9, Supporting Information). The spin Hamiltonian parameters of the ternary CuL(Aβ) species are compared with each of Cu(Aβ), CuL, and CuL_2 in Table 1.

To investigate the coordinating ligands of the ternary complex, we also obtained CW-EPR spectra of Cu/L/Aβ 1:1:1 using the truncated Aβ6−14 peptide. At pH 6.9, the spectrum of the ternary complex identified using Aβ1−16 was also observed for Aβ6−14 (Figure S10, Supporting Information), as shown in Figure 6a,b, demonstrating that the interacting ligands crucial to the complex were located entirely within this region. We then replaced Aβ6−14 by His, and once again a similar ternary CuL(His) spectrum could be identified (Figures S11−S13, Supporting Information), as shown in Figure 6c indicating that only histidine coordination was required. Replacement of His with imidazole again revealed a similar ternary spectrum (Figure S14−S16, Supporting Information), as shown in Figure 6d, confirming the coordination of the imidazolate moiety in CuL(His). It is noteworthy that the ratio of $g_{\|}/A_{\|}$ = 157 cm for CuL(imid) falls well outside the normal range expected for square planar or tetragonal Cu^{2+} coordination (105−135 cm), suggesting a strong tetrahedral distortion of the Cu^{2+} coordination sphere.[59] However, this range was established for Cu^{2+}-bound synthetic and natural peptides and proteins rather than synthetic heteroaromatic ligands such as L. Indeed, DFT geometry optimizations (*vide infra*) showed little indication for any significant tetrahedral distortion.

Although EPR spectroscopy provided unambiguous evidence for ternary CuLX formation with imidazolate-based ligands X, we also examined changes in the UV−vis spectrum upon titrating 1−20 equiv of imid into a solution containing Cu/L 1:1 (Figure 6g). During this titration, no evidence of charge transfer bands associated with free L was apparent near 240 nm (position a), nor was there any significant intensity change of LMCT transitions at 260 nm (position b) and 365 nm (position d). This indicated that Cu remained bound to L in an equimolar ratio even in the presence of 20 equiv imid, conditions under which CW-EPR indicated that a new species accounting for >90% of the bound Cu had formed. Spectra of free imid and $Cu(imid)_4$ did not exhibit significant absorbance in the range 230−1000 nm (Figure 6g). This new species did not correspond to CuL or CuL_2, or $Cu(imid)_4$ (Figure S15,

dx.doi.org/10.1021/ic302289r | *Inorg. Chem.* 2013, 52, 4303−4318

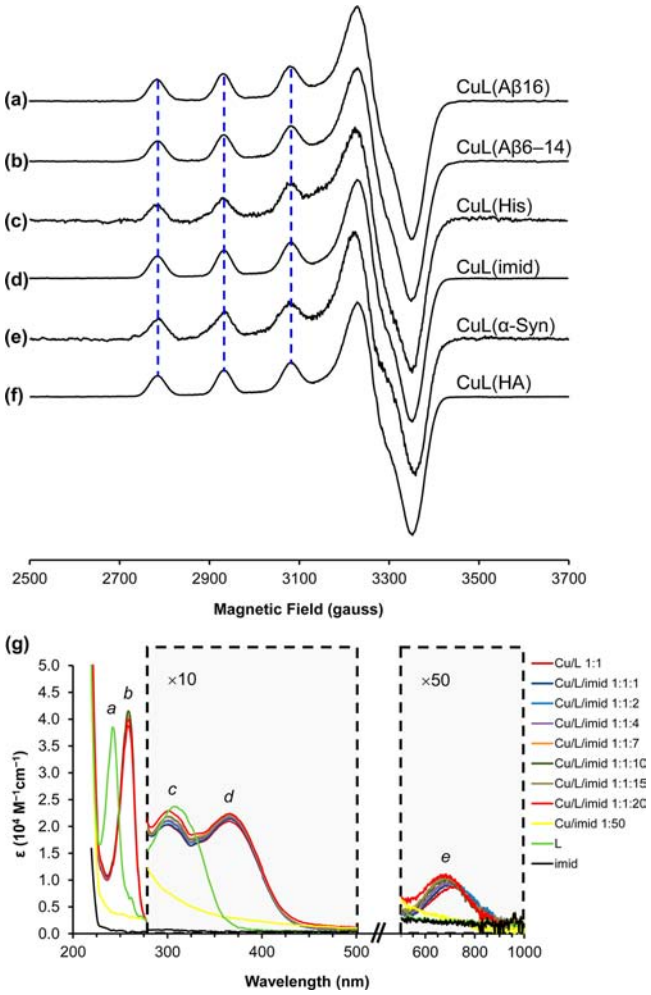

Figure 6. Comparison of the CW-EPR spectra of ternary CuLX species isolated from Cu/L/X 1:1:*n* spectra, with X = (a) Aβ16, (b) Aβ6–14, (c) His, (d), imid, (e) α-Syn, (f) HA. Dashed vertical lines are provided as a guide to the eye for comparison of the resolved $A_{\|}(^{65}Cu)$ hyperfine lines. (g) UV–vis absorption spectra following the titration of 0–20 equiv imid into a solution of CuL. The short wavelength spectra were acquired at [Cu] = 10 μM, while the control "L" and "imid" spectra were obtained at [L] = 10 μM and [imid] = 100 μM. The dashed boxes correspond to the spectra obtained at [Cu] = 100 μM, while the control "L" and "imid" spectra were obtained at [L] = 100 μM and [imid] = 1 mM.

Supporting Information). Additional evidence from UV–vis spectrophotometry for the formation of CuL(imid) could be obtained from the hypsochromic shift of the d–d transitions (position e), arising from the stronger ligand field of N_{Im} in CuL(imid) versus the Cl^-/phenolate ligand in CuL/CuL_2.

Since only the imidazolate group of a protein side chain was required, we determined whether a ternary CuL(His) complex could therefore form in the presence of *any* His-bearing protein side chain. Indeed, using the 140 amino acid protein α-synuclein (α-Syn), which contains a single His residue at position 50, we again isolated a ternary $CuL(His)_{\alpha\text{-Syn}}$ species in the CW-EPR spectrum of Cu/L/α-Syn 1:1:1 at pH 6.9 (Figure S17, Supporting Information), as shown in Figure 6e. Thus, although we have demonstrated that 2-substituted H8Qs can modulate Cu^{2+}/Aβ interactions *via* ternary complex formation, as proposed for PBT2,[11] this type of behavior is not unique to Aβ and ternary species may be formed more generally with any protein or peptide containing histidine.

Cu^{2+} Coordination of Mixtures of L with Peptides and Neurotransmitters. Given that L readily forms mixed ligand Cu^{2+} complexes with His *via* its imidazolate group, this suggested that HA, a neurotransmitter synthesized from His by the action of histidine decarboxylase,[60] can also act as a coligand of Cu^{2+}-bound L. Indeed, Figure 7 shows that titration of HA into equimolar Cu/L in PBS pH 6.9 led to the formation of a ternary CuL(HA) spectrum with the same appearance as CuL(Aβ), CuL(His), and CuL(imid), affirming the monodentate coordination of the aromatic group of HA. HYSCORE spectroscopy of Cu/L/HA 1:1:20, using an analogue of L containing ^{13}C-labeled *N*,*N*-dimethyl carbon atoms, revealed ^{13}C cross correlation ridges consistent with the coordination of the exocyclic amine of L (Figure 8a). Since only ternary CuL(HA) and binary $Cu(HA)_2$ species existed at the above stoichiometry (Figure 9d), the observed ^{13}C signals indicated that the exocyclic amine coordinates in the ternary CuL(HA) complex. The remaining cross-peaks near ~1.5 MHz and ~4 MHz arise from the distal nitrogen of the coordinating imidazolate group of HA and originate from the presence of both CuL(HA) and $Cu(HA)_2$ species in solution (Figure 9d). Geometry optimizations based upon terdentate coordination of L and monodentate HA coordination led to the structure shown in Figure 8b. The Cu–N_{Im} bond length was 1.95 Å, significantly shorter than the 2.00 bond length expected for most Cu-imid complexes. This is consistent with the bond shortening expected for ternary complexes involving heteroaromatic nitrogen bases due to π back-bonding.[3,6,61] Optimization of the CuL(imid) complex produced a structure with a different orientation of the imidazolate plane (Figure 8c), as expected due to steric constraints on the HA side chain; however, the first coordination sphere, to which CW-EPR is most sensitive, was not significantly altered. This explains the almost identical appearance of the CuL(Aβ), CuL(His), CuL(imid), and CuL(HA) spectra (Figure 6).

Figure 9 compares the distribution diagram produced from the deconvolution of the HA titration with those obtained from Aβ16, His, and imid titrations. The percentage of CuX_i species formed for X = His, HA, and imid at high X stoichiometries is consistent with the relative ordering of their stability constants.[48] For Aβ16, imid, and HA, the ternary complex predominated over a wider range of stoichiometries.

Titration of the neurotransmitters Y = Glu and Gly into an equimolar mixture of Cu/L revealed the presence of another putative ternary CuLY complex, as demonstrated for Glu in Figure 10. Using weighted spectral subtractions, the spectrum of the ternary species could be isolated (Figures S21–S23, Supporting Information). The CuL(Glu) spectrum (Figure 10e) was similar to, but distinct from, the spectra corresponding to the binary $Cu(Glu)_2$ complex (Figure 10g), with differences manifesting in the width and position of the $A_{\|}(^{65}Cu)$ resonances, together with differences in the $g_{\perp}$ region of the spectrum near 3300 G. As shown in Figure 11, comparable ternary spectra were obtained in the presence of Gly (Figure S24, Supporting Information), as well as other amino acids such as Trp (Figures S25–S27, Supporting Information) and Tyr (Figure S28, Supporting Information). In all instances, linear combinations of spectra corresponding to CuY_2 and CuL/CuL_2 failed to adequately reproduce the spectra in the Cu/L/Y 1:1:*n* titration. The comparable ternary CuLY spectra isolated in each instance indicated that the identity of

dx.doi.org/10.1021/ic302289r | *Inorg. Chem.* 2013, 52, 4303–4318

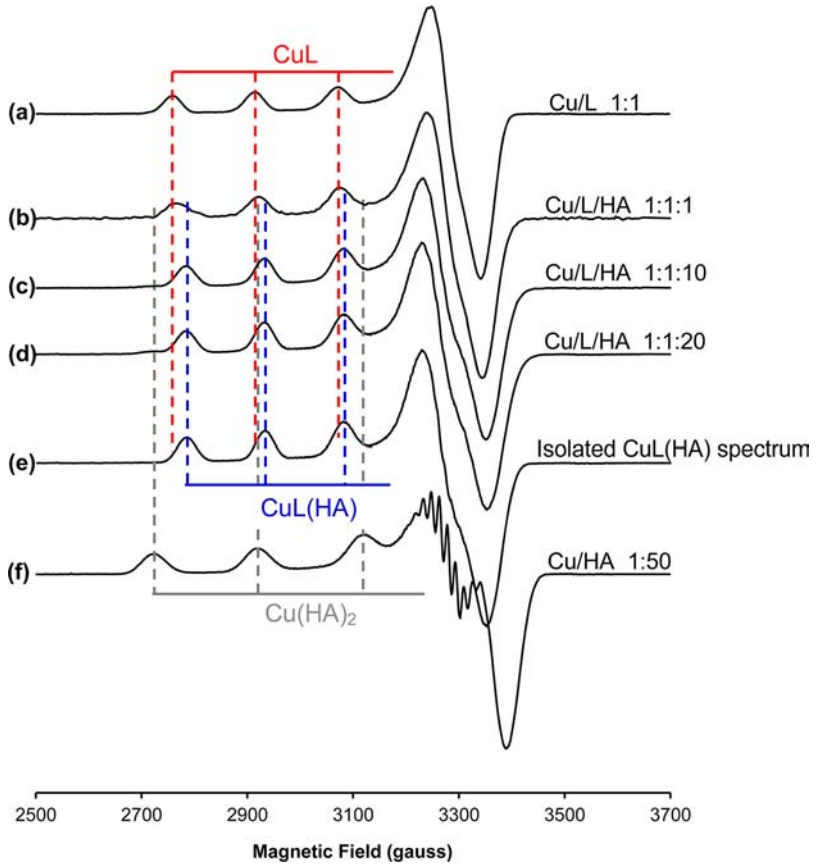

Figure 7. X-band (9.45 GHz) CW-EPR spectra showing the formation of the same ternary complex as in Figure 5 upon titrating 1−20 equiv HA into equimolar Cu/L in PBS 6.9. (a) Cu/L 1:1, (b) Cu/L/HA 1:1:1, (c) Cu/L/HA 1:1:10, (d) Cu/L/HA 1:1:20, (e) CuL(HA) spectrum, isolated as shown in Figure S18 (Supporting Information), (f) Cu/HA 1:50, yielding pure $Cu(HA)_2$. Vertical dashed lines indicate the positions of the resolved $A_{\|}(^{65}Cu)$ hyperfine lines for each species; for clarity, only CuL is indicated, although CuL_2 species are also present. A complete HA titration is provided in Figure S19 (Supporting Information).

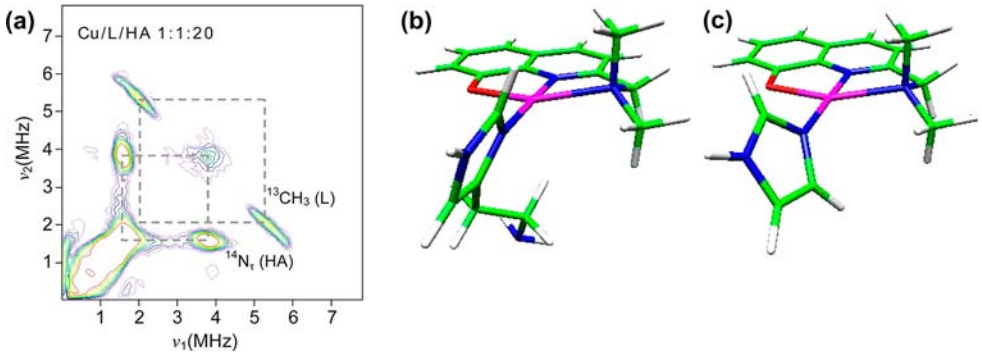

Figure 8. (a) X-band (9.70 GHz) HYSCORE spectrum (τ = 144 ns) of Cu/L/HA 1:1:20, obtained at 3370 G (near $g_{\perp}$) with ^{13}C labels on the carbons of the exocyclic amine of L. Since the CuL and CuL_2 species are negligibly populated at this stoichiometry (Figure 9d), the ^{13}C correlation ridges centered upon the ^{13}C Larmor frequency (3.71 MHz at 3370 G) with a splitting of ca. 3.3 MHz confirm the coordination of the exocyclic amine of L in CuL(HA). Additional cross-peaks attributable to the distal nitrogen of coordinating imidazole (predominantly from CuL(HA), but also due to $Cu(HA)_2$) are also present. (b, c) Energy-optimized structure of $[CuL(HA)]^+$ and $[CuL(imid)]^+$ satisfying the constraints imposed by CW-EPR and HYSCORE, depicting terdentate coordination of L in a 5,5-membered chelate ring, together with monodentate imidazolate coordination. Color definitions: pink, Cu^{2+}; blue, N; green, C; red, O; white, H.

the amino acid side chain does not greatly influence the geometric and electronic structure of the first coordination sphere, to which CW-EPR is most sensitive. The similarity of the CuY_2 and CuLY spectra (Figure 10) further indicated that both L and Y ligands of the ternary CuLY complex coordinated *via* 5-membered rings in a bidentate fashion, similar to the usual bis complexes adopted by amino acids. To confirm this, we replaced Glu, Trp, and Tyr with GABA, tryptamine (TA), and dopamine (DA), respectively, each of which lacks the carboxylate group. As expected, this abolished CuLY and yielded only CuL coordination (Figure 10h; Figures S26, S28, Supporting Information), consistent with the "glycine-like" bidentate coordination via both the carboxylate and amino groups of Y.

dx.doi.org/10.1021/ic302289r | *Inorg. Chem.* 2013, 52, 4303−4318

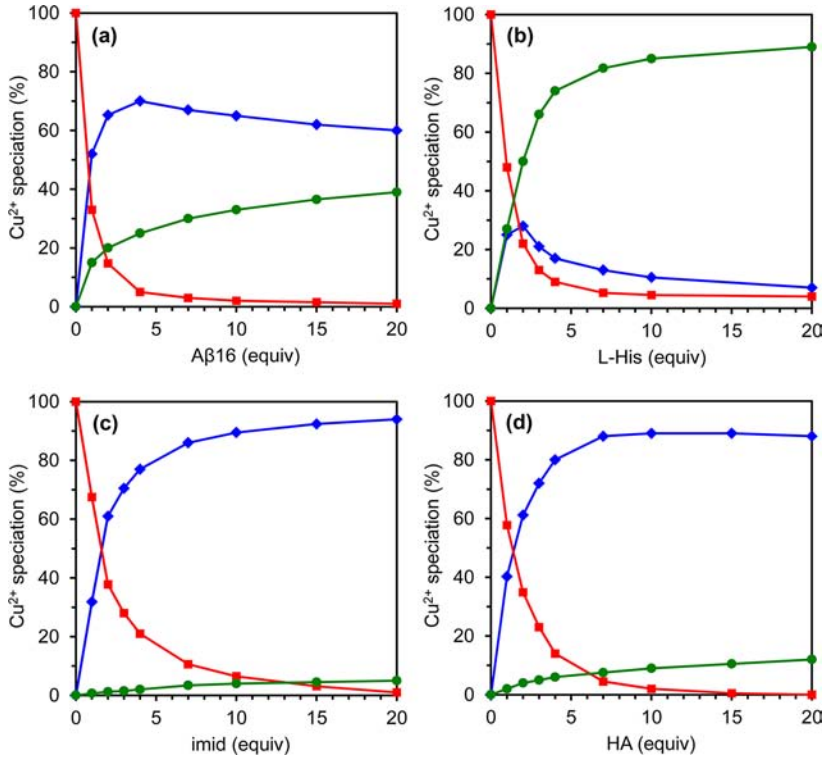

Figure 9. Distribution diagrams of complexes formed by Cu/L/X 1:1:*n* system as a function of ligand X stoichiometry *n*. Blue diamonds: CuLX. Red squares: ΣCuL_i, i = 1,2 (species I–III). Green circles: CuX_i. (a) X = Aβ, i = 1; (b) X = His, i = 2; (c) X = imid, i = 4; (d) X = HA, i = 1,2. The percentages were determined by decomposing the EPR spectra corresponding to each condition into linear combinations of binary and ternary Cu^{2+} spectra. The relative weightings of species I–III for a given Cu/L ratio were determined using the distribution diagram of Figure 3b.

Additional support for the assignment of a CuLY species was obtained by examining the changes in the UV–vis spectrum of Cu/L 1:1 upon titrating in 1–20 equiv of Trp (Figure 11h). During the titration, a bathochromic shift of the L→Cu charge transfer transition at 365 nm was observed (position d), together with hyperchromic shift in the range 400–500 nm (position d′). Examination of the spectra of L, CuL_i (Figure 1), Trp, and $Cu(Trp)_2$ indicated that only the latter had non-negligible absorbance between 400–500 nm; however, this was too low to account for the above spectral changes, indicating they were not the result of a simple exchange of Cu between L and Trp.

To confirm the bidentate coordination of L in CuLY complexes, we obtained HYSCORE spectra of Cu/L/Trp 1:1:20, conditions under which the speciation is almost pure CuL(Trp) (Figure 12). In contrast to the case observed for CuL(HA) (Figure 8a), site-specific ^{13}C-labeling of the exocyclic amine of L failed to reveal any ^{13}C cross-peaks in CuL(Trp) (Figure 13a), confirming that the ternary CuLY species does not involve terdentate coordination of L. This also verified that the LMCT transition at 365 nm (Figure 11f) is due to charge transfer from the π-conjugated ring substituents of L.

Titration with ligands containing sulfur groups, namely the tripeptide γ-Glu-Cys-Gly (glutathione; GSH) and L-methionine (Met), did not produce ternary complexes involving sulfur coordination. In the case of Met, a spectrum corresponding to a CuL(Met) complex similar to that adopted by other amino acids was obtained (Figure 11e; Figure S29, Supporting Information), with no evidence of participation from the thioether side group. Not surprisingly, in the presence of GSH, an EPR-silent cuprous GSSG complex resulted following the rapid one-electron reduction of Cu^{2+} by the cysteine thiol group of GSH.[62] When the oxidized form of glutathione (glutathione disulfide; GSSG) was used, a spectrum corresponding to a ternary CuL(GSSG) complex analogous to other CuLY was observed (Figure 11f; Figure 30, Supporting Information) due to the coordination of the N-terminal glutaminyl moiety of GSSG in a "glycine-like" fashion (as found also in Cu(GSSG) complexes).[62]

Finally, we ascertained that a similar ternary CuLY species could be adopted by 8HQs lacking a coordinating moiety at position 2 by demonstrating that sulfoxine could form a comparable ternary Cu(sulfoxine)(Trp) complex (Figure S31, Supporting Information), as indicated by the similar CW-EPR spectrum shown in Figure 11g. These findings are consistent with previous reports that amino acids can form ternary divalent metal complexes, both with other amino acids and with aromatic ligands.[3,4,63]

Geometry optimizations based upon bidentate coordination of L and Y led to distorted square-planar CuLY structures, as shown in Figure 13b,c for Y = Glu and Trp. It is noteworthy that, in the presence of X = His, a different complex of the form shown in Figure 8b,c was adopted, indicating that ternary complexes involving terdentate coordination of L with monodentate coligands containing imidazolate groups (e.g., HA) are more stable than those involving bidentate coordination of L and its coligands (e.g., Glu, GSSG). This conclusion was further confirmed by a competition experiment in which 20 equiv of both HA and Glu were added to an equimolar Cu/L mixture. The CW-EPR spectrum of Cu/L/Glu/HA 1:1:20:20 revealed the presence of predominantly CuL(HA), together with a second unique species ascribed to Cu(HA)(Glu), and a control spectrum of Cu/HA/Glu 1:20:20 also yielded the same unique Cu(HA)(Glu) species (Figure

dx.doi.org/10.1021/ic302289r | Inorg. Chem. 2013, 52, 4303–4318

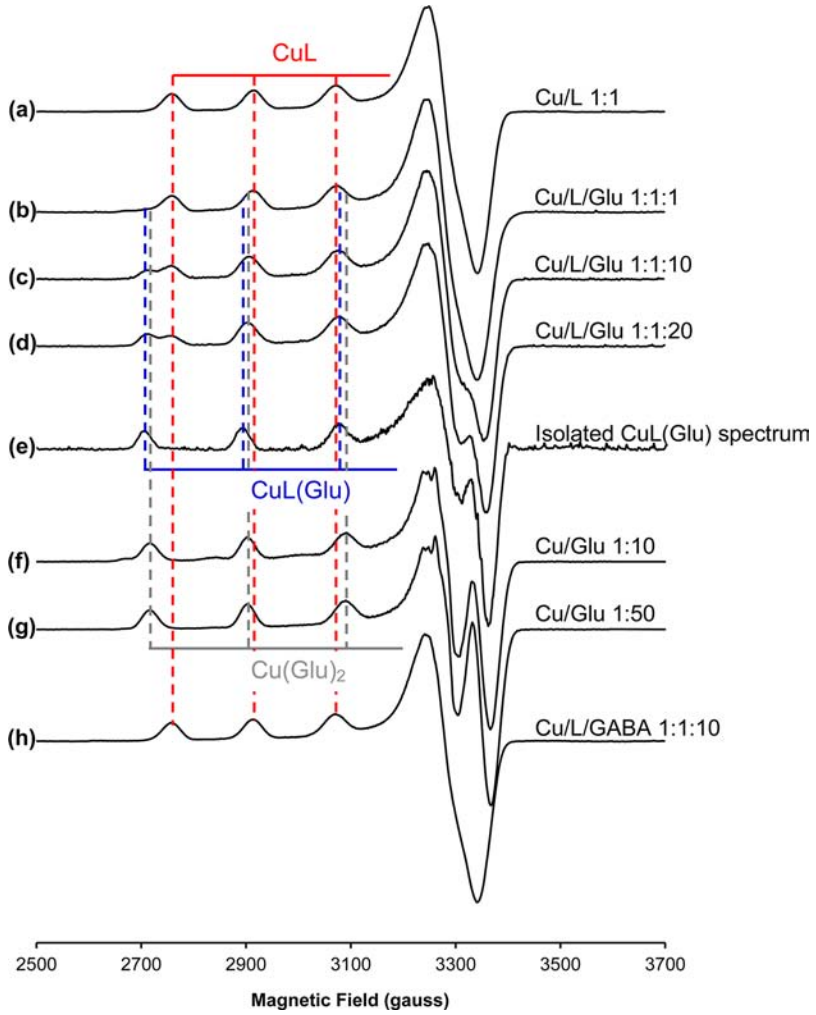

Figure 10. X-band (9.450 GHz) CW-EPR spectra showing the formation of a ternary complex upon titrating 1−20 equiv of Glu into equimolar Cu/L in PBS 6.9. (a) Cu/L 1:1, (b) Cu/L/Glu 1:1:1, (c) Cu/L/Glu 1:1:10, (d) Cu/L/Glu 1:1:20, (e) CuL(Glu) spectrum, isolated as shown in Figure S21 (Supporting Information), (f) Cu/Glu 1:10, (g) Cu/Glu 1:50, yielding pure $Cu(Glu)_2$, (h) Cu/L/γ-aminobutyric acid 1:1:10, yielding only CuL. Vertical dashed lines indicate the positions of the resolved $A_{\parallel}(^{65}Cu)$ hyperfine lines for each species; for clarity, only CuL is indicated, although CuL_2 species are also present. A complete Glu titration is provided in Figure S22 (Supporting Information).

S32, Supporting Information). No CuL(Glu) was detectable, indicating that CuL(Glu) is less stable than CuL(HA), which is consistent with the species distribution plots (cf. Figures 9 and 12).

DISCUSSION

Copper is one of the most tightly regulated metals in the body; however, the synapse represents the one place where there is likely to be sufficient exchangeable copper, with high concentrations of Cu being released during neurotransmission.[28,29] This study has therefore focused upon likely coligands that may be encountered at the synapse, especially those relevant to AD, such as the neurotransmitters Glu and HA, as well as the Aβ peptide. It has been demonstrated that such mixed-ligand Cu^{2+} complexes can indeed be formed by L, some of which are unique to this class of 8HQ due to its ability to act as a terdentate metal ligand. Although it is difficult to predict the type of complexes that will be formed by L and other homologues in it class, it should be clear that, given the number of coligands available in the biological milieu, a variety of mixed-ligand complexes will be possible. Importantly, these ternary Cu^{2+} complexes will predominate strongly over binary metal complexes, and in a biological environment, the CuL and CuL_2 species are unlikely to be formed in most instances.

Our findings indicate that L has a strong capacity to act as a multifunctional ligand, which has direct consequences for the therapeutic applications of the homologous ligand PBT2 that forms the same Cu^{2+} complexes (Figure S33, Supporting Information). Two main functions have so far been proposed for PBT2 as an AD therapeutic, including (i) the prevention of deleterious Cu^{2+}/Aβ interactions and (ii) the promotion of intracellular metal ion transport, thereby activating neuroprotective signaling cascades. With respect to the first function, a ternary Cu(PBT2)(Aβ) complex can help redox-silence Aβ by reducing accessibility to its binary Cu^{2+} coordination modes, which involve multiple His ligands.[52] Ternary Cu(PBT2)(Aβ) interactions have previously been proposed in this context,[11,13] but our results provide a molecular basis for such interactions. The cortex of AD patients contains insoluble Aβ concentrations of the order 200 μg/g and soluble Aβ concentrations of the order 100 pg/g.[64] In Tg2576 mice, insoluble and soluble Aβ concentrations have been measured at ∼600 μg/g and ∼35−40 μg/g, respectively, and basal Aβ levels in the interstitial fluid of APP/PS1 mice have been measured at 2 μg/L (∼50 nM).[13]

dx.doi.org/10.1021/ic302289r | Inorg. Chem. 2013, 52, 4303−4318

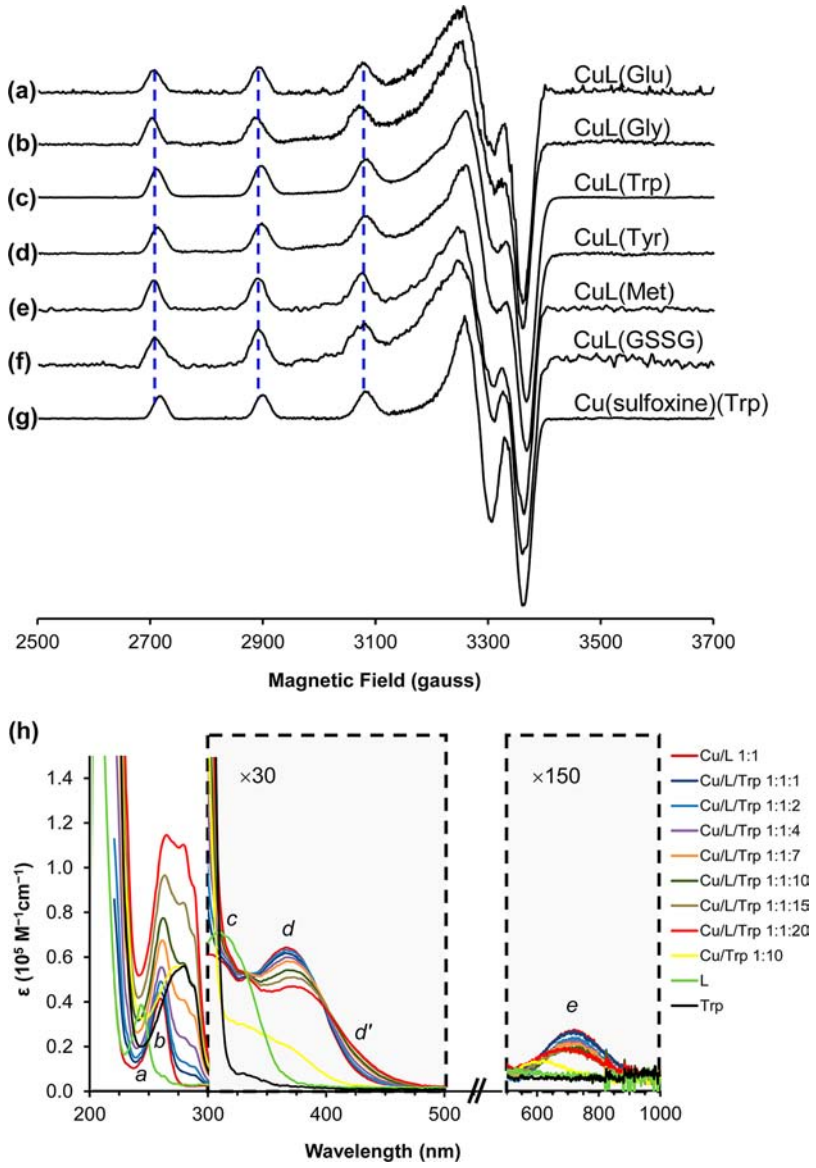

Figure 11. Comparison of the ternary CuLY species isolated from Cu/L/Y 1:1:*n* spectra, with X = (a) Glu, (b) Gly, (c) Trp, (d) Tyr, (e) Met, (f) _GSSG. For comparison, the ternary spectrum isolated from Cu^{2+}/sulfoxine/Trp 1:1:10 is shown in part g, indicating that this type of mixed-ligand species can be formed by other 8HQs lacking 2-substitution. Dashed vertical lines are provided as a guide to the eye for comparison of the resolved $A_{\parallel}(^{65}Cu)$ hyperfine lines. (h) UV−vis absorption spectra following the titration of 0−20 equiv Trp into a solution of CuL. The short wavelength spectra were acquired at [Cu] = 10 μM, while the control "L" and "Trp" spectra were obtained at [L] = 10 μM and [Trp] = 100 μM, respectively. The dashed boxes correspond to the spectra obtained at [Cu] = 100 μM, while the control "L" and "Trp" spectra were obtained at [L] = 100 μM and [Trp] = 1 mM, respectively.

This compares with measured brain concentrations of PBT2 of ~300 ng/g in Tg2756 mice two hours after oral administration at 30 mg/kg, with a clearance from the interstitial fluid within 12 h.[13] Thus, the concentration of ligand remains modest compared with both Cu^{2+} and Aβ levels.

With regard to the second proposed function of PBT2, the addition of 10 μM Cu/PBT2 1:1 has been shown to increase intracellular Cu levels by almost 4000% in cultured M17 human neuroblastoma cells;[13] however, such extreme metal chaperone activity is not readily apparent from animal data, leading to the suggestion that PBT2 could act mostly on translocating metal ions localized in metal-rich amyloid plaques, which account for a very small percentage of the total brain mass and are unlikely to lead to gross changes total tissue metal levels.[13] Nevertheless, our EPR data indicate that ternary interactions will not be restricted to hyper-metalated Aβ. Given the excess of available His side chains *in vivo*, metal chaperone activity via passive diffusion or pinocytosis of neutral bis complexes across cell membranes is unlikely. Indeed, ternary Cu(PBT2)(xx-His-yy) complexes involving coordination of protein His side chains (xx,yy = any amino acids), with subsequent disassociation and release of Cu^{2+} upon reaching a low-pH and/or reducing intracellular environment, provide a general means for the observed increase in intracellular copper levels as a consequence of protein endocytosis. The reported superiority of PBT2 compared with CQ in promoting uptake of divalent copper and zinc[13] may result from the ability of PBT2 to form specific ternary structures of the form shown in Figure 8, which are inaccessible to CQ because it lacks the coordinating exocyclic amine.

dx.doi.org/10.1021/ic302289r | *Inorg. Chem.* 2013, 52, 4303−4318

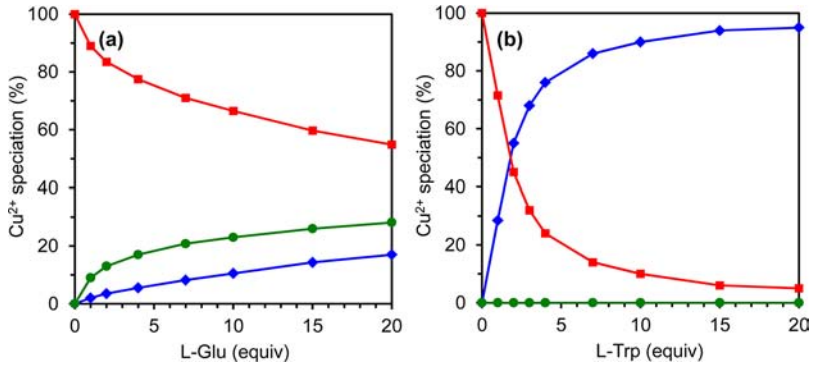

Figure 12. Distribution diagrams of complexes formed by Cu/L/Y 1:1:*n* system as a function of ligand X stoichiometry *n*. Blue diamonds: CuLY. Red squares: ΣCuL_i, i = 1,2 (species I–III). Green circles: CuY_i. (a) Y = Glu, Σi = 1,2; (b) Y = Trp, i = 2. The percentages were determined by decomposing the EPR spectra corresponding to each condition into linear combinations of binary and ternary Cu^{2+} spectra. The relative weightings of species I–III for a given Cu/L ratio were determined using the distribution diagram of Figure 3b.

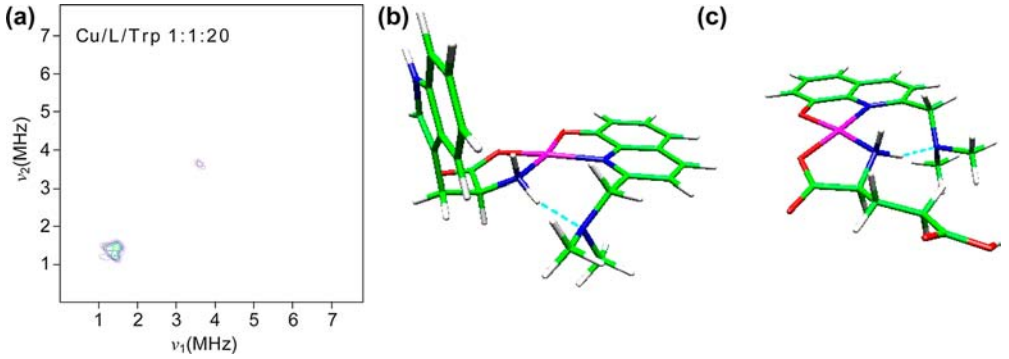

Figure 13. (a) X-band (9.70 GHz) HYSCORE spectrum (τ = 144 ns) of Cu/L/Trp 1:1:20, obtained at 3370 G (near $g_\perp$), with ^{13}C labels on the carbons of the exocyclic amine of L. Since the CuL and CuL_2 species are negligibly populated at this stoichiometry (Figure 12b), the absence of ^{13}C correlation ridges confirms the exocyclic amine of L does not coordinate in CuL(Trp). (b, c) Energy-optimized structures of $[CuL(Trp)]^0$ and $[CuL(Glu)]^0$ complexes satisfying the constraints imposed by CW-EPR and HYSCORE, depicting bidentate coordination of both L and amino acids via 5-membered chelate rings. Color definitions: pink, Cu^{2+}; blue, N; green, C; red, O; white, H; dashed aqua line, hydrogen bond.

The functional consequences of increased intracellular metal levels may depend upon the identity of the protein providing the His coligand, which could determine the delivery of Cu^{2+} to a specific subcellular compartment. In the case of neurotransmitter coligands such as HA and Glu, ternary CuL(HA) and CuL(Glu) complexes might be recognized and actively transported during monoamine reuptake. The released ligands could be degraded or repackaged into synaptic vesicles for recycling. Reuptake of Glu is accomplished by a family of five different Na^+-dependent high-affinity glutamate transporters, including EAAT1 and EAAT2.[65] In the case of HA, the reuptake mechanism remains more obscure.[66,67] The metal binding affinity of the ligand L will also have functional implications, since this will determine the extent to which His residues binding Cu^{2+} ions in functional protein active sites are disrupted in order to form a CuL(xx-His-yy) species. Such disruption is known to occur for other metal ions and other substituted 8HQs, most notably 5-substituted 8HQs, which can form a ternary complex at the active site Fe^{2+} center of 2-oxoglutarate-dependent histone demethylase.[9]

Besides redox-silencing of Cu/Aβ interactions and metal chaperone activity, our data suggest other putative actions of this class of 8HQ ligand arising from the ternary interactions with neurotransmitters and Cu^{2+} that are released at the synapse. Within the CNS, HA modulates many physiological responses in humans, including wakefulness and attention, and induces long-term potentiation (LTP) in the hippocampus, a major mechanism underlying learning and memory.[68,69] These actions are mediated via four G-protein-coupled receptors (GPCR) named H1–H4 with various second messenger pathways.[69] There is good evidence that H3 receptors influence learning and memory by modulating the release of other neurotransmitters such as acetylcholine and Glu,[68,69] making the HA system a prime therapeutic target for the treatment of cognitive disorders. The action of HA on H1 and H2 receptors effects signaling pathways distinct from H3, which include promoting neural stem cell differentiation and proliferation, respectively.[70,71] H3 antagonist-evoked neurotransmitter release leads to activation of other postsynaptic receptor pathways such as phosphorylation of glycogen synthase kinase 3 (GSK-3), a constitutively active kinase involved in the regulation of a wide array of cellular functions, including apoptosis, and microtubule assembly/disassembly (including tau hyperphosphorylation in AD).[72] Inactivation (by phosphorylation of Ser9) or pharmacological inhibition of GSK-3 leads to both increased proliferation and enhanced neurogenesis in neural stem cell cultures.[73] Notably, the L homologue PBT2 has been shown to induce GSK-3β phosphorylation in a human neuroblastoma cell line[21] and increased neurite outgrowth in a mouse model of AD.[14] Although H3 receptor expression is significantly lower in mice compared with humans and rats,[74] it is interesting to speculate that these effects could be mediated by the antagonism of H3 receptors by a Cu(PBT2)(HA)

dx.doi.org/10.1021/ic302289r | Inorg. Chem. 2013, 52, 4303–4318

complex, or by its interference with the extracellular histamine methyltransferase (the primary HA inactivation mechanism).[69]

While no disease of the CNS has been attributed solely to perturbed histaminergic neurotransmission, statistically significant decreases in HA concentrations have been observed in the hippocampus (−57%), the temporal cortex (−47%), and the hypothalamus of AD patients as compared with age-matched controls, who had typical HA concentrations of ∼0.4 nM/g wet weight in the hippocampus and temporal cortex and ∼5 nM/g in the hypothalamus.[75] Neurofibrillary tangles associated with AD are also found in the tuberomammillary nucleus of the hypothalamus,[76] from where all histaminergic nerve endings project. The role of the brain HA system in learning and memory and in facilitating neuroregeneration makes it an attractive target on which ternary complexes of L homologues may act.

Glutamate is the principal excitatory neurotransmitter in the mammalian CNS and activates a family of ligand-gated ion channels (NMDA, AMPA, kainate) and a family of metabotropic GPCRs (mGluR1−8).[77,78] The level of Glu is extremely high in the mammalian CNS, although only a very small fraction of this is extracellular. While there is no consensus, the peak Glu concentration attained in the synaptic cleft following release is likely in the low millimolar range prior to diffusion into the extracellular space, where Glu concentrations are normally around 3−4 μM in the extracellular fluid[77] and the cerebrospinal fluid (CSF).[79] Consequentially, many glutamate receptors are activated by low micromolar (1−10 uM) Glu concentrations, but excess extracellular Glu (10−100 μM in cultured neurons) causes overactivation of Glu receptors, leading to elevated intracellular Ca^{2+} levels and subsequent cell death (excitotoxicity).[65] Concentrations as low as 1 μM are neurotoxic if Glu uptake is blocked.[77]

Significantly higher levels of Glu have been detected in the CSF of patients with AD as compared with aged-matched controls.[79] A number of observations implicate Aβ-related changes in the glutamate system to progression of AD, including increases in Glu release, decreases in Glu uptake by astrocytes, and prolonged activation of NMDA receptors, leading not only to excitotoxicity but enhanced Aβ production.[78] Aβ-induced dendritic spine loss, LTP inhibition, and induction of long-term depression have also been observed in AD pathology and can be related to perturbations of the Glu system.[78] In this context, it is noteworthy that PBT2 and CQ both significantly reverse the Aβ-induced inhibition of LTP in the CA1 region of hippocampal slices from APP/PS1 mice[13] and protect against deficits in spine density of Tg2756 mice.[14] Although it remains unclear how Aβ modulates NMDA receptor function,[78] the protection afforded by these 8HQs might be at least partially be explained by the formation of Cu(PBT2)(Glu) and Cu(CQ)(Glu) complexes similar to those shown in Figure 13, either by antagonizing NMDA receptors or preventing Glu binding to the agonist site. Of course, additional protection against Aβ-mediated potentiation of Glu excitotoxicity might also arise from the formation of a CuL(Aβ) complex. Analogous conclusions also apply to Gly, since ternary CuL(Gly) complexes with affinity comparable to CuL(Glu) can also be formed (cf. Figures S21 and S24, Supporting Information), and Gly acts as a coagonist of NMDA receptors.[80] Typical Gly concentrations of ∼10 μM are present in human CSF[79] and extracellular fluid (microdialysis),[80] and significantly higher levels of Gly have been detected in the CSF of patients with AD as compared with aged-matched controls.[79] Moreover, there is some evidence that Aβ can act as an agonist at the glycine binding site of the NMDA receptor,[81] and once again such action could be inhibited by formation of a CuL(Aβ) complex.

It is notable that histaminergic and glutamatergic systems are not independent. For example, HA binds to the polyamine modulatory site to directly facilitate NMDA receptors, and binding of HA to H3 heteroreceptors also modulates the release of other neurotransmitters including Glu.[69] Hence, antagonism by CuL(HA) of either H3 heteroreceptors to inhibit Glu release or of the polyamine site of NMDA receptors to reduce Aβ-induced excitotoxicity is also plausible.

Similar to Glu and Gly, the tripeptide GSSG forms a ternary CuL(GSSG) complex. Glutathione is the most abundant low molecular weight peptide in eukaryotic cells, where it serves as a key antioxidant, with additional roles in cell metabolism and cell cycle.[82] GSH is present at concentrations in the range of 1−10 mM and approximately 1% of total intracellular glutathione is in the oxidized glutathione disulfide form (GSSG) under basal conditions; however, under conditions characterized by oxidative stress, intracellular GSH is rapidly depleted leading to increased levels of GSSG, some of which is actively transported out of the cell.[82,83] An elevated GSSG/GSH ratio has been measured in the peripheral blood from AD patients,[84] in the hippocampus of individuals with mild cognitive impairment (those who usually progress to AD)[85] and both immediately before and following the onset of amyloid plaques in the cerebrum, cerebellum, and hippocampus of a double transgenic mouse model of AD.[86] Increased intracellular GSSG levels are potently toxic to mouse hippocampal HT4 neuronal cells.[87] Of more significance to a potential role for cupric CuL(GSSG) complex, extracellular GSSG has also been reported to induce apoptotic cell death (*via* a p38 MAP kinase pathway) in proliferating U937 cells.[88] Although the relevance of this finding to a neuronal lineage is uncertain, sequestering GSSG in a ternary CuL(GSSG) complex could interfere with extracellular GSSG-mediated toxicity.

■ CONCLUSIONS

This study demonstrates for the first time that CuLX interactions involving coligands such as X = Aβ, xx-His-yy, HA, Glu, Gly, and GSSG can be formed by the family of ligands homologous to L, principally the AD therapeutic PBT2. Complexes with X = Aβ, xx-His-yy, HA involve terdentate coordination of L, together with monodentate coordination of the hetetoaromatic nitrogen of X. Complexes with Y = Glu, Gly, and GSSG involve bidentate coordination of L via its imino and phenolato groups and bidentate coordination of Y via its amino and carboxylato groups. No ternary complexes are formed with tryptamine- (e.g., serotonin, melatonin), and tyramine-based (e.g., dopamine) neurotransmitters, or GABA, each which lack the required carboxylato moiety. Ternary CuLX and CuLY complexes could play a multifunctional role in the treatment of AD by mediating translocation of Cu^{2+}, antagonizing Cu/Aβ interactions and by modulating neurotransmission with potential neuroprotective and neuroregenerative effects. Further research to determine the *in vivo* relevance of these complexes is warranted.

dx.doi.org/10.1021/ic302289r | *Inorg. Chem.* 2013, 52, 4303−4318

■ ASSOCIATED CONTENT

Supporting Information

Potentiometric data, additional EPR spectra, spectral deconvolutions, geometry-optimized structures in xyz format. This material is available free of charge via the Internet at http://pubs.acs.org.

■ AUTHOR INFORMATION

Corresponding Author

*E-mail: sdrew@unimelb.edu.au.

Notes

The authors declare the following competing financial interest(s): K.J.B. and C.L.M. are consultants and shareholders in Prana Biotechnology.

■ ACKNOWLEDGMENTS

This work was supported by a Future Fellowship (S.C.D.) administered by the Australian Research Council and a Program Grant administered by the National Health and Medical Research Council of Australia (K.J.B., C.L.M). K.J.B. is an NHMRC Senior Research Fellow. Peptide synthesis was carried out by John Karas in the Peptide Technology Facility of the Bio21 Molecular Science and Biotechnology Institute, The University of Melbourne. The α-synuclein protein was kindly provided by Roberto Cappai, The University of Melbourne. The potentiometric equipment used was sponsored by the Centre for Preclinical Research and Technology (CePT), a project cosponsored by European Regional Development Fund and Innovative Economy, The National Cohesion Strategy of Poland.

■ REFERENCES

(1) Stevenson, R. L.; Freiser, H. *Anal. Chem.* **1967**, *39*, 1354−1358.
(2) Hata, T.; Uno, T. *Bull. Chem. Soc. Jpn.* **1972**, *45*, 477−481.
(3) Sigel, H. *Angew. Chem., Int. Ed. Engl.* **1975**, *14*, 394−402.
(4) Marcus, Y.; Eliezer, I. *Coord. Chem. Rev.* **1969**, *4*, 273−322.
(5) Sundberg, R. J.; Martin, B. *Chem. Rev.* **1974**, *74*, 471−517.
(6) Sigel, H.; Martin, R. B. *Chem. Rev.* **1982**, *82*, 385−426.
(7) Burns, C. J.; Field, L. D.; Hambley, T. W.; Lin, T.; Ridley, D. D.; Turner, P.; Wilkinson, M. P. *ARKIVOC* **2001**, No. vii, 157−165.
(8) Mancin, F.; Chin, J. *J. Am. Chem. Soc.* **2002**, *124*, 10946−10947.
(9) King, O. N.; Li, X. S.; Sakurai, M.; Kawamura, A.; Rose, N. R.; Ng, S. S.; Quinn, A. M.; Rai, G.; Mott, B. T.; Beswick, P.; Klose, R. J.; Oppermann, U.; Jadhav, A.; Heightman, T. D.; Maloney, D. J.; Schofield, C. J.; Simeonov, A. *PLoS One* **2010**, *5*, e15535.
(10) Rajagopalan, R.; Archilefu, S. I.; Bugaj, J. E.; Dorshow, R. B. *Quinoline Ligands and Metal Complexes for Diagnosis and Therapy*. United States Patent 6277841 B1, Aug. 21, 2001.
(11) Bush, A. I.; Tanzi, R. E. *Neurotherapeutics* **2008**, *5*, 421−432.
(12) Kenche, V. B.; Barnham, K. J. *Br. J. Pharmacol.* **2011**, *163*, 211−219.
(13) Adlard, P. A.; Cherny, R. A.; Finkelstein, D. I.; Gautier, E.; Robb, E.; Cortes, M.; Volitakis, I.; Liu, X.; Smith, J. P.; Perez, K.; Laughton, K.; Li, Q.-X.; Charman, S. A.; Nicolazzo, J. A.; Wilkins, S.; Deleva, K.; Lynch, T.; Kok, G.; Ritchie, C. W.; Tanzi, R. E.; Cappai, R.; Masters, C. L.; Barnham, K. J.; Bush, A. I. *Neuron* **2008**, *59*, 43−55.
(14) Adlard, P. A.; Bica, L.; White, A. R.; Nurjono, M.; Filiz, G.; Crouch, P. J.; Donnelly, P. S.; Cappai, R.; Finkelstein, D. I.; Bush, A. I. *PLoS One* **2011**, *6*, e17669.
(15) Lannfelt, L.; Blennow, K.; Zetterberg, H.; Batsman, S.; Ames, D.; Harrison, J.; Masters, C. L.; Targum, S.; Bush, A. I.; Murdoch, R.; Wilson, J.; Ritchie, C. W. *Lancet Neurol.* **2008**, *7*, 779−86.
(16) Barnham, K. J.; Gautier, E. C. L.; Kok, G. B.; Krippner, G. *8-Hydroxy Quinoline Derivatives*. United States Patent 2006/0089380 A1, Apr. 27, 2006.
(17) Telpoukhovskaia, M. A.; Orvig, C. *Chem. Soc. Rev.* **2012**, *42*, 1836−1846.
(18) The symbol L will henceforth be used to describe both the protonated and deprotonated form of L, with the meaning being clear from the context. Similar usage also applies to all other ligands described in this work.
(19) Treiber, C.; Simons, A.; Strauss, M.; Hafner, M.; Cappai, R.; Bayer, T. A.; Multhaup, G. *J. Biol. Chem.* **2004**, *50*, 51958−51964.
(20) Schafer, S.; Pajonk, F.-G.; Multhaup, G.; Bayer, T. *J. Mol. Med.* **2007**, *85*, 405−413.
(21) Bareggi, S. R.; Cornelli, U. *CNS Neurosci. Ther.* **2010**, DOI: 10.1111/j.1755-5949.2010.00231.x.
(22) Crouch, P. J.; Savva, M. S.; Hung, L. W.; Donnelly, P. S.; Mota, A. I.; Parker, S. J.; Greenough, M. A.; Volitakis, I.; Adlard, P. A.; Cherny, R. A.; Master, C. L.; Bush, A. I.; Barnham, K. J.; White, A. R. *J. Neurochem.* **2011**, *119*, 220−230.
(23) Cherny, R. A.; Atwood, C. S.; Xilinas, M. E.; Gray, D. N.; Jones, W. D.; McLean, C. A.; Barnham, K. J.; Volitakis, I.; Fraser, F. W.; Kim, Y.; Huang, X.; Goldstein, L. E.; Moir, R. D.; Lim, J. T.; Beyreuther, K.; Zheng, H.; Tanzi, R. E.; Masters, C. L.; Bush, A. I. *Neuron* **2001**, *30*, 665−676.
(24) Ritchie, C. W.; Bush, A. I.; Mackinnon, A.; Macfarlane, S.; Mastwyk, M.; MacGregor, L.; Kiers, L.; Cherny, R.; Li, Q. X.; Tammer, A.; Carrington, D.; Mavros, C.; Volitakis, I.; Xilinas, M.; Ames, D.; Davis, S.; Beyreuther, K.; Tanzi, R. E.; Masters, C. L. *Arch. Neurol.* **2003**, *60*, 1685−1691; Erratum: *Arch Neurol.* **2004**, *61*, 776.
(25) Bush, A. I. *Neurobiol. Aging* **2002**, *23*, 1031−1038.
(26) Deraeve, C.; Pitie, M.; Meunier, B. *J. Inorg. Biochem.* **2006**, *100*, 2117−2126.
(27) Rózga, M.; Protas, A. M.; Jabłonowska, A.; Dadlez, M.; Bal, W. *Chem. Commun.* **2009**, 1374−1376.
(28) Hartter, D. E.; Barnea, A. *Synapse* **1988**, *2*, 412−415.
(29) Kardos, J.; Kovács, I.; Hajós, F.; Kálmán, M.; Simonyi, M. *Neurosci. Lett.* **1989**, *103*, 139−144.
(30) Drew, S. C.; Noble, C. J.; Masters, C. L.; Hanson, G. R.; Barnham, K. J. *J. Am. Chem. Soc.* **2009**, *131*, 1195−1207.
(31) Drew, S. C.; Masters, C. L.; Barnham, K. J. *J. Am. Chem. Soc.* **2009**, *131*, 8760−8761.
(32) Drew, S. C.; Masters, C. L.; Barnham, K. J. *PLoS One* **2010**, *5*, e15875.
(33) Drew, S. C.; Leong, S. L.; Pham, C. L. L.; Tew, D. J.; Masters, C. L.; Miles, L. A.; Cappai, R.; Barnham, K. J. *J. Am. Chem. Soc.* **2008**, *130*, 7766−7773.
(34) Hassani, M.; Cai, W.; Holley, D. C.; Lineswala, J. P.; Maharjan, B. R.; Ebrahimian, G. R.; Seradj, H.; Stocksdale, M. G.; Mohammadi, F.; Marvin, C. C.; Gerdes, J. M.; Beall, H. D.; Behforouz, M. *J. Med. Chem.* **2005**, *48*, 7733−7749.
(35) Konovalov, V. V.; Zvanut, M. E. *Phys. Rev. B* **2003**, *69*, 012102.
(36) Hanson, G. R.; Gates, K. E.; Noble, C. J.; Griffin, M.; Mitchell, A.; Benson, S. *J. Inorg. Biochem.* **2004**, *98*, 903−916.
(37) Schweiger, A.; Jeschke, G. *Principles of Pulse Electron Paramagnetic Resonance*; Oxford University Press: Oxford, 2001; p 107, 165.
(38) Irving, H.; Miles, M. G.; Pettit, L. D. *Anal. Chim. Acta* **1967**, *38*, 475−488.
(39) Gans, P.; Sabatini, A.; Vacca, A. *Talanta* **1996**, *43*, 1739−1753.
(40) Neese, F. *ORCA—An ab Initio, DFT and Semiempirical SCF-MO Package, Version 2.8, Revision 20*; University of Bonn: Bonn, Germany, 2010.
(41) Becke, A. D. *Phys. Rev. A* **1988**, *38*, 3098−3100.
(42) Perdew, J. P. *Phys. Rev. B* **1986**, *33*, 8822−8824.
(43) Schäfer, A.; Horn, H.; Ahlrichs, R. *J. Chem. Phys.* **1992**, *97*, 2571−2577.
(44) R. Ahlrichs and co-workers, unpublished.
(45) *gOpenMol for Windows, v. 3.00*; 2005; http://www.csc.fi/gopenmol/UT.
(46) Ferrada, E.; Arancibia, V.; Loeb, B.; Norambuena, E.; Olea-Azar, C.; Huidobro-Toro, J. P. *NeuroToxicology* **2007**, *28*, 445−449.

(47) Di Vaira, M.; Bazzicalupi, C.; Orioli, P.; Messori, L.; Bruni, B.; Zatta, P. *Inorg. Chem.* **2004**, *43*, 3795−3797.
(48) Dawson, R. M.; Elliot, D. C.; Elliot, W. H.; Jones, K. M. *Data for Biochemical Research*, 3rd ed.; Clarendon Press: Oxford, 1990; pp 404−405.
(49) Walter, E. D.; Chattopadhyay, M.; Millhauser, G. L. *Biochemistry* **2006**, *45*, 13083−13092.
(50) Coughlin, P. K.; Lippard, S. J. *Inorg. Chem.* **1984**, *23*, 1446−1451.
(51) Fiallo, M. M. L.; Garnier-Suillerot, A. *J. Inorg. Biochem.* **1987**, *31*, 43−55.
(52) Drew, S. C.; Barnham, K. J. *Acc. Chem. Res.* **2011**, *44*, 1146−1155.
(53) Pogni, R.; Baratto, M. C.; Busi, E.; Basosi, R. *J. Inorg. Biochem.* **1999**, *73*, 157−165.
(54) Peisach, J.; Blumberg, W. E. *Arch. Biochem. Biophys.* **1974**, *165*, 691−698.
(55) Schosseler, P. M.; Wehrli, B.; Schweiger, A. *Inorg. Chem.* **1997**, *36*, 4490−4499.
(56) Brändén, R.; Deinum, J. *FEBS Lett.* **1977**, 144−146.
(57) Lohmann, W.; Fowler, C. F.; Moss, A. J., Jr.; Perkins, W. H. *Cell. Mol. Life Sci.* **1965**, *21*, 31−32.
(58) Chang, R. *Physical Chemistry with Application to Biological Systems*, 2nd ed.; Macmillan Publishing Co.: New York, 2001; p 345.
(59) Pogni, R.; Baratto, M. C.; Busi, E.; Basosi, R. *J. Inorg. Biochem.* **1999**, *73*, 157−165.
(60) Darvas, Z.; Falus, A. "Histidine decarboxylase (HDC) enzyme and gene. In *Histamine: Biology and Medical Aspects*; Falus, A., Ed.; SpringMed Publishing: Budapest, 2004; pp 31−42.
(61) Nair, M. S.; Santappa, M.; Natarajan, P. *J. Chem. Soc., Dalton Trans.* **1980**, 1312−1316.
(62) Pedersen, J. Z.; Steinkühler, C.; Weser, U.; Rotilio, G. *BioMetals* **1996**, *9*, 3−9.
(63) Yamauchi, O. *Pure Appl. Chem.* **1995**, *67*, 297−304.
(64) Lue, L. F.; Kuo, Y. M.; Roher, A. E.; Brachova, L.; Shen, Y.; Sue, L.; Beach, T.; Kurth, J. H.; Rydel, R. E.; Rogers, J. *Am. J. Pathol.* **1999**, *155*, 853−862.
(65) Sheldon, A. L.; Robinson, M. B. *Neurochem. Int.* **2007**, *51*, 333−355.
(66) Sakurai, E.; Sakurai, E.; Oreland, L.; Nishiyama, S.; Kato, M.; Watanabe, T.; Yanai, K. *Pharmacology* **2006**, *78*, 72−80.
(67) Perdan-Pirkmajer, K.; Mavri, J.; Kržan, M. *J. Mol. Model.* **2010**, *16*, 1151−1158.
(68) Passani, M. B.; Lin, J.-S.; Hancock, A.; Crochet, S.; Blandina, P. *Trends Pharmacol. Sci.* **2004**, *25*, 618−625.
(69) Haas, H.; Panula, P. *Nat. Rev. Neurosci.* **2003**, *4*, 121−130.
(70) Molina-Hernández, A.; Velasco, I. *J. Neurochem.* **2008**, *106*, 706−717.
(71) Rodríguez-Martínez, G.; Velasco, I.; García-Lopez, G.; Solís, K. H.; Flores-Herrera, H.; Díaz, N. F.; Molina-Hernández, A. *Neuroscience* **2012**, *216*, 10−17.
(72) Brioni, J. D.; Esbenshade, T. A.; Garrison, T. R.; Bitner, S. R.; Cowart, M. D. *J. Pharmacol. Exp. Ther.* **2011**, *336*, 38−46.
(73) Lange, C.; Mix, E.; Frahm, J.; Glass, Ä.; Müller, J.; Schmitt, O.; Schmöle, A.-C.; Klemm, K.; Ortinau, S.; Hübner, R.; Frecha, M. J.; Wree, A.; Rolfs, A. *Neurosci. Lett.* **2011**, *488*, 36−40.
(74) Nuutinen, S.; Panula, P. *Adv. Exp. Med. Biol.* **2010**, *709*, 95−107.
(75) Panula, P.; Rinne, J.; Kuokkanen, K.; Eriksson, K. S.; Sallmen, T.; Kalimo, H.; Relja, M. *Neuroscience* **1998**, *82*, 993−997.
(76) Airaksinen, M. S.; Reinikainen, K.; Riekkinen, P.; Panula, P. *Agents Actions* **1991**, *33*, 104−107.
(77) Danbolt, N. C. *Prog. Neurobiol.* **2001**, *65*, 1−105.
(78) Revett, T. J.; Baker, G. B.; Jhamandas, J.; Kar, S. *J. Psychiatry Neurosci.* **2012**, *38*, 6−23.
(79) Jiménez-Jiménez, F. J.; Molina, J. A.; Gómez, P.; Vargas, C.; de Bustos, F.; Benito-León, J.; Tallón-Barranco, A.; Ortí-Pareja, M.; Gasalla, T.; Arenas, J. *J. Neural Transm.* **1998**, *105*, 269−277.
(80) Danysz, W.; Parsons, C. G. *Pharmacol. Rev.* **1998**, *50*, 597−664.
(81) Cowburn, R. F.; Wiehager, B.; Trief, E.; Li-Li, M.; Sundström, E. *Neurochem. Res.* **1997**, *22*, 1437−1442.
(82) Denke, S. M.; Fanburh, B. L. *Am. J. Physiol.* **1989**, *257*, L163−L173.
(83) Meister, M.; Anderson, M. E. *Annu. Rev. Biochem.* **1983**, *52*, 711−760.
(84) Calabrese, V.; Sultana, R.; Scapagnini, G.; Guagliano, E.; Sapienza, M.; Bella, R.; Kanski, J.; Pennisi, G.; Mancuso, C.; Stella, A. M. G.; Butterfield, D. A. *Antioxid. Redox Signaling* **2006**, *8*, 1975−1986.
(85) Sultana, R.; Piroddi, M.; Galli, F.; Butterfield, D. A. *Neurochem. Res.* **2008**, *33*, 2540−2546.
(86) Zhang, C.; Rodriguez, C.; Spaulding, J.; Aw, T. Y.; Feng, J. *J. Alzheimer's Dis.* **2012**, *28*, 655−666.
(87) Park, H.-A.; Khanna, S.; Rink, C.; Gnyawali, S.; Roy, S.; Sen, C. K. *Cell Death Differ.* **2009**, *16*, 1167−1179.
(88) Filomenti, G.; Rotilio, G.; Ciriolo, M. R. *FASEB J.* **2003**, *17*, 64−66.